Current Research in Toxicology 2 (2021) 1–18

Contents lists available at ScienceDirect

Current Research in Toxicology

journal homepage: www.elsevier.com/locate/crtox

In utero and lactational PCB exposure drives anatomic changes in the juvenile mouse bladder

Kimberly P. Keil Stietz [a,b,*], Conner L. Kennedy [b], Sunjay Sethi [a], Anthony Valenzuela [a], Alexandra Nunez [b], Kathy Wang [b], Zunyi Wang [c], Peiqing Wang [c], Audrey Spiegelhoff [b], Birgit Puschner [a], Dale E. Bjorling [c], Pamela J. Lein [a]

[a] Department of Molecular Biosciences, University of California-Davis, School of Veterinary Medicine, Davis, CA, USA
[b] Department of Comparative Biosciences, University of Wisconsin-Madison, School of Veterinary Medicine, Madison, WI, USA
[c] Department of Surgical Sciences, University of Wisconsin-Madison, School of Veterinary Medicine, Madison, WI, USA

ARTICLE INFO

Keywords:
Developmental origins of health and disease
Persistent organic pollutants
Lower urinary tract
Peripheral nervous system
Polychlorinated biphenyls

ABSTRACT

Bladder dysfunction, including incontinence, difficulty emptying the bladder, or urgency to urinate is a pervasive health and quality of life concern. However, risk factors for developing these symptoms are not completely understood, and the influence of exposure to environmental chemicals, especially during development, on the formation and function of the bladder is understudied. Environmental contaminants such as polychlorinated biphenyls (PCBs) are known to pose a risk to the developing brain; however, their influence on the development of peripheral target organs, such as bladder, are unknown. To address this data gap, C57Bl/6J mouse dams were exposed to an environmentally-relevant PCB mixture at 0, 0.1, 1 or 6 mg/kg daily beginning two weeks prior to mating and continuing through gestation and lactation. Bladders were collected from offspring at postnatal days (P) 28–31. PCB concentrations were detected in bladders in a dose-dependent manner. PCB effects on the bladder were sex- and dose-dependent. Overall, PCB effects were observed in male, but not female, bladders. PCBs increased bladder volume and suburothelial βIII-tubulin-positive nerve density compared to vehicle control. A subset of these nerves were sensory peptidergic axons indicated by increased calcitonin gene-related protein (CGRP) positive nerve fibers in mice exposed to the highest PCB dose compared to the lowest PCB dose. PCB-induced increased nerve density was also positively correlated with the number of mast cells in the bladder, suggesting inflammation may be involved. There were no detectable changes in epithelial composition or apoptosis as indicated by expression of cleaved caspase 3, suggesting PCBs do not cause overt toxicity. Bladder volume changes were not accompanied by changes in bladder mass or epithelial thickness, indicating that obstruction was not likely involved. Together, these results are the first to suggest that following developmental exposure, PCBs can distribute to the bladder and alter neuroanatomic development and bladder volume in male mice.

1. Introduction

Bladder function is one of the major factors contributing to quality of life (Rubin et al., 2016). Common lower urinary tract symptoms (LUTS) for which patients seek clinical intervention include overactive bladder, painful urination/urinary tract infection, difficulty emptying the bladder, and nocturia (Kullmann et al., 2015). Bladder dysfunction occurs in both men and women, and while common in the aging population, children and individuals with neurodevelopmental disorders also suffer from LUTS (Kullmann et al. (2015); Santos et al. (2017); Sakakibara et al. (2008)). The diverse range of symptoms associated with bladder dysfunction suggests that factors contributing to their onset and severity are likely multifactorial. Whether environmental chemicals constitute a class of risk factors for bladder dysfunction is not well understood, but increasing evidence suggests that environmental factors influence the timing and progression of lower urinary tract dysfunction associated with prostate disease in mice (Nicholson et al., 2018; Ricke et al., 2016).

One class of environmental contaminants of concern are the polychlorinated biphenyls (PCBs), which are known to exert adverse effects on the developing central nervous system (Tsai et al., 2017; Lyall et al., 2017; Schantz et al., 2003). Although synthesis and use

* Corresponding author at: Department of Comparative Biosciences University of Wisconsin-Madison School of Veterinary Medicine, 2015 Linden Drive, Madison, WI 53706, USA.
E-mail address: kkeil@wisc.edu (K.P. Keil Stietz).

https://doi.org/10.1016/j.crtox.2021.01.002
Received 6 September 2020; Revised 16 December 2020; Accepted 5 January 2021

of PCBs was banned in the United States in the late 1970's, PCBs continue to be detected in serum and tissue from livestock (Sethi et al., 2017a; Chen et al., 2017) and humans (Lyall et al., 2017; Barmpas et al., 2020; Klocke et al., 2020; Schantz et al., 2010). This is largely attributed to their resistance to degradation, as well as continued exposure via products containing legacy PCBs, and exposure to unintentional byproducts from contemporary manufacturing processes, such as pigment production (Klocke et al., 2020; Hu and Hornbuckle, 2010). Humans are exposed to PCBs primarily via inhalation (Ampleman et al., 2015) and diet (Chen et al., 2017; Schantz et al., 2010; Ampleman et al., 2015; Marek et al., 2017; Stewart et al., 1999). PCBs can have adverse effects on the developing nervous system and are linked to impaired cognitive function in children exposed during early development (Lyall et al., 2017; Schantz et al., 2003; Eubig et al., 2010). In rodent models, one of the major modes of action of PCBs in the central nervous system is their ability to enhance dendritic complexity, which is in turn linked to decreased performance in learning and memory tasks (Wayman et al., 2012a, 2012b; Yang et al., 2009). However, PCB effects on peripheral targets and/or the peripheral nervous system are not well characterized.

Altered peripheral innervation and/or nerve function play a major role in the pathogenesis of LUTS and serve as therapeutic targets for symptomatic treatment (Radomski, 2014). Increased density of afferent sensory nerves expressing calcitonin-gene related peptide (CGRP) and substance P are observed in bladders from patients with detrusor instability compared to patients with no symptoms of frequency or urgency (Smet et al., 1997). Heightened sensitivity of bladder afferent nerves to stimuli also contributes to bladder symptoms (Arms and Vizzard, 2011; Birder et al., 2002; Cockayne et al., 2005; Schnegelsberg et al., 2010; Silva-Ramos et al., 2013). Thus, bladder innervation may be a target by which environmental chemicals act to alter bladder morphology and function.

PCB exposures have been identified as possible risk factors for neurodevelopmental disorders such as autism (Lyall et al., 2017; Schantz et al., 2003; Granillo et al., 2019; Pessah et al., 2019; Mitchell et al., 2012). Children with neurodevelopmental disorders are also at elevated risk of experiencing lower urinary tract symptoms such as incontinence (von Gontard et al., 2011, 2016, 2015a, 2015b; von Gontard and Equit, 2015; Gubbiotti et al., 2019a, 2019b). Observations that bladder dysfunction is a common comorbidity of several disorders linked to PCB exposure strongly support the need for further research in this area. Whether developmental exposure to PCBs contributes to changes in bladder structure or function has not yet been examined. As a first step in addressing this gap, we sought to test the hypothesis that developmental exposure to PCBs in mice, leads to morphological changes in bladder, which could contribute to bladder dysfunction. To test this hypothesis we employ the use of the novel PCB mixture termed the MARBLES (Markers of Autism Risk in Babies – Learning Early Signs) PCB mixture (Sethi et al., 2019; Rude et al., 2019), which mimics the composition of the most abundant congeners detected in the serum of women who are at risk of having a child with a neurodevelopmental disorder enrolled in the MARBLES study (Hertz-Picciotto et al., 2018).

2. Materials and methods

2.1. Animals

All procedures involving animals were conducted in accordance with the NIH Guide for the Care and Use of Laboratory Animals and were approved by the University of California-Davis Animal Care and Use Committee. C57BL/6J and SVJ129 wild type mice were purchased from Jackson Labs (Sacramento, CA) and crossed to generate a 75% C57BL/6J / 25% SVJ129 genetic background, which was determined by SNP analysis to match the genetic background of genotypes used previously (Keil et al., 2019). All mice were housed in clear plastic (H-TEMP Polysulfone) shoebox cages containing corn cob bedding and maintained on a 12 h light and dark cycle at 22 ± 2 °C. Feed (Diet 5058, LabDiet, Saint Louis, MO) and water (sterile filtered tap water in hydropacs) were available ad libitum.

2.2. Developmental PCB exposures

Organic peanut butter (Trader Joe's, Monrovia, CA) and organic peanut oil (Spectrum Organic Products, LLC, Melville, NY) were used to orally dose dams with PCB mixture. The PCB mixture includes the following PCB congeners in the specified proportion [PCB −28 (48.2%), −11 (24.3%), −118 (4.9%), −101 (4.5%), −52 (4.5%), −153 (3.1%), −180 (2.8%), −149 (2.1%), −138 (1.7%), −84 (1.5%), −135 (1.3%) and −95 (1.2%)] and is termed the MARBLES PCB mixture because it mimics the top congeners identified in serum from pregnant women enrolled in the MARBLES cohort (Granillo et al., 2019; Sethi et al., 2019; Hertz-Picciotto et al., 2018), a prospective study of pregnant women in California at increased risk of having a child with a neurodevelopmental disorder (Hertz-Picciotto et al., 2018). PCBs were synthesized and authenticated by the Synthesis Core of the University of Iowa Superfund Research Program with >99% purity as reported previously (Sethi et al., 2019). PCBs were dissolved in peanut oil, and then homogenously mixed into peanut butter using a bullet blender. Two weeks prior to mating, nulliparous dams were fed PCBs mixed in peanut butter daily at doses of either 0, 0.1, 1.0 or 6.0 mg/kg/day. These doses were chosen for several reasons. First, single PCB congeners or other Aroclor mixtures at these doses have been shown to result in offspring displaying behavioral abnormalities including deficits in learning/memory and altered dendrite morphology (Wayman et al., 2012b; Yang et al., 2009; Kania-Korwel et al., 2017; Klocke and Lein, 2020). This allows for the comparison between our endpoints and behavioral outcomes (Klocke and Lein, 2020). Second, in rodents, these doses lead to levels of PCBs in tissues of developmentally exposed offspring that generally recapitulate the range of levels observed in animal and human samples (Yang et al., 2009; Klocke and Lein, 2020; Chu et al., 2003; Li et al., 2019; Dewailly et al., 1999; Covaci et al., 2002). Dams were then paired with a male. Dams continued to be dosed daily throughout mating, gestation and lactation. After weaning at postnatal day (P) 21 (last day of lactational PCB exposure), offspring were group housed with other littermates of the same sex receiving the same dose, prior to collection of tissues at P28-31. Animals were not fasted prior to collection and were collected by individuals blinded to treatment groups throughout the day across several collection days in a random order, so that not all animals from a litter were collected consecutively.

2.3. Bladder PCB measurement

Following CO_2 euthanasia, whole bladders were removed and immediately stored at −80 °C until analyzed. A 50 mg aliquot of pooled bladder tissue was removed, placed in a microtube, and homogenized in 800 μl acetonitrile using a Geno/Grinder bead homogenizer (SPEX SamplePrep LLC, Metuchen, NJ, USA). After tissue homogenization, the tubes were vortexed, sonicated, and mechanically shaken to facilitate extraction of PCBs. Samples were then centrifuged, and the supernatant collected. The remaining pellet was resuspended and extracted twice more using a 50/50 solution of acetonitrile and isopropanol; 600 μl of the solution were used for the second extraction and 400 μl for the third. During each subsequent extraction, the tubes were vortexed, sonicated, shaken, centrifuged, and the supernatant collected. The three supernatants were filtered through a Phree Phospholipid Removal Plate (Phenomenex Inc., Torrance, CA, USA) to remove proteins and phospholipids and then combined. The combined supernatant was evaporated under nitrogen, reconstituted in 50 μl isooctane, and centrifuged to remove any

residue. The resulting supernatant was loaded into an auto-sampler vial for GC/EI-MS/MS analysis.

An eight-point calibration curve at PCB concentrations of 2.5, 5, 10, 20, 30, 40, 60 and 80 ng/g was prepared by adding PCB analytical standards (AccuStandard Inc., New Haven, CT, USA) to 50 mg of brains derived from mice that had not been exposed to PCBs. Quality control (QC) samples with PCBs added at concentrations of 12.5, 25, and 50 ng/g were prepared in the same way. Calibrators and QCs, as well as matrix blanks and reagent blanks, were processed following the same extraction method as samples. All samples, calibrators, QCs, and blanks were internal standard-corrected with a 13C-labeled PCB 97 internal standard (Cambridge Isotope Laboratories Inc., Tewksbury, MA, USA) at a concentration of 100 ng/g. Extracted samples were analyzed as previously described (Sethi et al., 2017c; Lin et al., 2013) using a Bruker Scion triple quadruple mass spectrometer equipped with a Scion 456-GC and CP-8400 auto-sampler and series split/splitless injector (Bruker Scientific LLC, Billerica, MA, USA). The standard curve matrix used brain tissue since this method was developed for brain tissue, however this extraction method also worked well for bladders, therefore bladder tissue was run in the same method as brain tissue. Additionally, brain tissues from these mice are part of a larger study analyzing PCBs in brain tissue as a forthcoming publication.

2.4. Immunohistochemistry

Following CO_2 euthanasia, whole bladders were fixed in 4% paraformaldehyde (Sigma St. Louis, MO, w/v diluted in phosphate buffered saline) overnight, dehydrated in methanol and stored at −20 °C. Samples were rehydrated, embedded in paraffin, and sectioned to 5 μm thickness. Multiple bladders from each PCB exposure group were embedded within the same block to ensure the same region (mid-bladder) was examined across groups and to decrease variability in staining. Immunohistochemistry was performed on bladder sections as described previously (Abler et al., 2011) using antibodies listed in Table 2. Images were captured using an Eclipse E600 or Eclipse Ci compound microscope (Nikon Instruments Inc., Melville, NY) with a Photometrics Dyno CCD camera or DS Ri2 camera (Nikon Instruments Inc.) interfaced to NIS elements imaging software (Nikon Instruments Inc.). Imaged areas were selected based on the DAPI or pan-epithelial marker, E-cadherin, channel (i.e. not the channel used for analysis) to eliminate bias. Multiple images (at least 2–3; encompassing the top, middle and bottom of the section) were acquired per bladder and averaged for analysis. Nerve density was quantified using Image J as described (Turco et al., 2019). Briefly, within Image J, the entire stroma or muscle was outlined and saved in the region of interest manager tool within Image J for analysis. For the suburothelium, a region 10 μm thick was drawn along the entire epithelial border labeled by E-cadherin and saved for analysis. The nerve fiber channel alone was then opened, a threshold applied and the area of positive pixels within the saved regions was measured using the analysis-measure feature of Image J. The threshold remained constant for the entire batch of images. Quantification of cells positive for keratin 5 (KRT 5) and transforming related protein 63 (P63) as epithelial differentiation markers, and cleaved caspase 3 as an apoptotic marker, were performed by an experimenter blinded to group using the cell counter function in Image J as described (Joseph et al., 2018). Epithelial thickness was determined in KRT 5 positive basal epithelium, KRT 20 superficial epithelium, and total epithelium (base of KRT 5 layer to top of KRT 20 layer) using the line tool within Image J with three regions (randomly selected from the top, middle and bottom of the section) measured per bladder section and averaged for final value. Mast cells were stained with Toluidine blue (Sigma). Slides were deparaffinized and rehydrated through ethanol washes. A 1% w/v toluidine blue stock solution was prepared in 70% ethanol. Toluidine blue working solution was prepared from stock solution, 5 ml into 45 ml of 1% sodium chloride, pH 2.3. Slides were placed in working solution for 3 min, washed, dehydrated and coverslipped. Mast cells were quantified in all cell layers of the entire bladder section by 2–3 individuals blinded to conditions, averaged, and normalized to bladder area. Hematoxylin (Gills, Fisher Scientific, Pittsburgh, PA) and eosin (Sigma) stain was performed using described methods (Joseph et al., 2018). Bladder muscle thickness was quantified in images of hematoxylin and eosin stained bladder sections. The line tool within Image J was used to measure the distance from 5 muscle regions spaced across the entire bladder section, these regions were averaged for one final value for each bladder as described (Joseph et al., 2018).

2.5. Bladder and urine metrics

Free catch urine was collected into a microcentrifuge tube while mice were gently scruffed. Urine was collected ~between 10AM and 3PM, 1–2 days prior to euthanasia and frozen. Urine was analyzed using commercially available kits according to the manufacturer's instructions for creatinine (Creatinine Kit 80350, Crystal Chem, Elk Grove, Il) and protein (Pierce BCA 23225, ThermoFisher, Waltham, MA). Following CO_2 euthanasia, but prior to removing the bladder, bladder volume was measured using a digital caliper and the volume calculated as described previously (Nicholson et al., 2012). Bladder volume measurements were conducted in a blinded manner.

2.6. Statistics

Data were analyzed using GraphPad Prism 6. Significant differences in concentrations of specific PCB congeners between PCB-exposed animals and vehicle control were determined using Kruskal-Wallis test followed by Dunn's multiple comparisons tests. For summary statistics, samples with non-detectable values were assigned a value 1/2 the limit of detection (LOD). Pearson r was used to assess correlations. For all other endpoints, normality was assessed using the KS normality test, homogeneity of variance was determined using Bartlett's test or Brown-Forsythe test. Data were transformed (log(y)) if necessary. A one-way ANOVA followed by Tukey's multiple comparisons tests were used to determine significant differences between experimental groups for males and for females. If transformation did not normalize or result in equal variance, Kruskal-Wallis test followed by Dunn's multiple comparisons tests were used to determine significant differences between groups. If data were normal but had unequal variance Welch's one-way ANOVA test followed by Dunnett T3 post hoc test was used to determine significant differences between groups. p values ≤ 0.05 were considered significant. Tests used are indicated in figure legends. Sample sizes are indicated in each figure legend and samples were obtained from at least 3 independent litters.

3. Results

3.1. PCBs are detected in bladder tissue of weanling mice exposed to PCB developmentally

We first sought to determine whether PCBs are distributed to the bladder of postnatal day (P) 28–31 male mice following developmental exposure to the MARBLES PCB mix in the maternal diet throughout gestation and lactation at 0, 0.1, 1, or 6 mg/kg/d, and whether the sum total of detectable PCBs increases with increasing doses. Table 1 summarizes mean abundance of PCBs in male bladder of P28-P31 mice – which corresponds to 7–10 days after the last possible lactational PCB exposure. 9 of the 12 congeners were above the limit of detection in at least one sample. There was a significant increase in the sum total of detectable PCBs in the 1 mg/kg and 6 mg/kg dose groups compared to vehicle control (Fig. 1; $H_3 = 11.1$, $p = 0.0002$). Individually, PCBs 28, 52, 118, 138, 153, and 180 were greater in the 1 and 6 mg/kg

Table 1
Mean PCB concentrations in male offspring bladder tissue (ng/g).

Limit of Detection (LOD)	PCB Congener	[MARBLES PCB mg/kg/d via dam]			
		0	0.1	1	6
0.096	PCB11	3.42 ± 1.73	1.48 ± 0.21	1.85 ± 0.61	1.85 ± 0.85
0.183	PCB28	1.71 ± 1.62	36.45 ± 15.46	202.62 ± 36*	599.24 ± 313.59*
0.192	PCB52	0.45 ± 0.36	4.95 ± 1.79	18.54 ± 2.27*	60.36 ± 46.34*
0.441	PCB84				
0.469	PCB95	0.234 ± 0	0.234 ± 0	0.68 ± 0.44	0.234 ± 0
0.300	PCB101	0.28 ± 0.13	2.43 ± 0.91	10.46 ± 2.04*	24.09 ± 23.09
0.500	PCB118	0.66 ± 0.41	23.70 ± 7.95	119.81 ± 10.14*	811.80 ± 359.49*
1.714	PCB135				
0.472	PCB138	0.31 ± 0.08	6.91 ± 1.81	35.76 ± 4.65*	235.13 ± 102.24*
0.714	PCB149				
0.418	PCB153	0.43 ± 0.22	20.40 ± 6.27	103.12 ± 10.53*	607.21 ± 264.27*
0.385	PCB180	0.45 ± 0.26	9.80 ± 2.78	53.63 ± 3.76*	309.58 ± 129.67*
	∑PCBs	7.95 ± 2.20	106.35 ± 36.25	546.47 ± 35.30*	2649.51 ± 1216.75*

Results are mean ± SEM, n = 3–4 pools of bladder tissue per group, for summary statistics samples which had values that were not detected were assigned 1/2 the LOD value. *Indicates statistically significant from vehicle control $p \leq 0.05$ as determined by Kruskal-Wallis test with Dunn's post hoc analysis. Empty cells indicate that congener was not detected above the stated LOD for any of the samples.

Table 2
Antibodies used in this study.

Primary Antibodies		Source	Company		Catalog #	Dilution
Beta-III tubulin		Mouse	Abcam		ab78078	1:250
Calcitonin gene related peptide (CGRP)		Mouse	Abcam		ab81887	1:200
E-cadherin (CDH1)		Rabbit	Cell Signaling		3195s	1:250
Keratin 5		Chicken	Biologend		905901	1:500
Keratin 20		Mouse	Dako		M701929-2	1:300
Transformation related protein 63 (P63) (4A4)		Mouse	Biocare Medical		CM163 A	1:200
Uroplakin III		Mouse	Fitzgerald		10R-U103a	1:50
Cleaved caspase 3 (Asp 175)		Rabbit	Cell Signaling Technology		9661S	1:200
Secondary Antibodies					Paired with primary antibody	
Anti-Mouse Alexa Fluor 488	Donkey	Jackson ImmunoResearch	715-585-150	1:250	Beta-III tubulin	
Anti-Mouse Alexa Fluor 594	Donkey	Jackson ImmunoResearch	715-545-150	1:250	P63, Keratin 20, Uroplakin III, CGRP	
Anti-Rabbit Alexa Fluor 488	Donkey	Jackson ImmunoResearch	711-545-152	1:250	E-cadherin	
Anti-Rabbit Alexa Fluor 594	Goat	Jackson ImmunoResearch	111-516-045	1:250	Cleaved caspase 3, E-cadherin	
Anti-Chicken Alexa Fluor 488	Donkey	Jackson ImmunoResearch	703-546-155	1:250	Keratin 5	

treatment group compared to vehicle control (Table 1). PCB 101 showed a non-monotonic response and was only significantly higher in the 1 mg/kg dose group compared to vehicle control (Table 1). Of those detected, PCB 11 and PCB 95 were the only two which did not show a significant difference from control with increasing doses. This is likely due to the fact that PCB 95 is the lowest proportional PCB within the mixture and PCB 11, being a lower chlorinated congener, has a relatively short biological half-life which likely explains low levels and no difference across groups 7–10 days post last exposure.

3.2. Developmental PCB exposure does not induce apoptosis in bladder or alter bladder epithelial composition

PCBs have been linked to apoptosis in the brain (Yang and Lein, 2010) as well as in cultured neurons (Sanchez-Alonso et al., 2003), endothelial cells (Lee et al., 2003) and kidney cells (Ghosh et al., 2010). We, therefore, wanted to address whether PCBs similarly increase apoptosis in the bladder. Using cleaved caspase 3 as a marker to label apoptotic cells (Fig. 2A-B), few apoptotic cells were detected in bladder stroma and epithelium, and quantitative analyses revealed no significant differences between groups (Fig. 2C-D; (C) $F_{3,\ 18} = 0.3$, $p = 0.8$, (D) $F_{3,\ 18} = 0.08$, $p = 1$).

Bladder formation and development in mice occur between embryonic days 9.5–14 (Georgas et al., 2015). Since mice were exposed to PCBs throughout this developmental programming period, we sought to determine whether PCB exposure alters the cellular composition of the bladder urothelium. Previous studies have characterized three cell populations that make up the urothelium based on their expression of unique markers (Joseph et al., 2018; Georgas et al., 2015; Gandhi et al., 2013). Using a combination of basal (Keratin 5, KRT5, green) and basal + intermediate (transforming related protein 63, P63, red) markers (Fig. 3A-B) we found that PCBs do not alter the percentage of total epithelial cells that are basal (KRT5 + P63 +) (Fig. 3C-D; (C) $F_{3,\ 17} = 0.3$, $p = 0.8$, (D) $W_{3,\ 7.8} = 1.1$, $p = 0.4$), intermediate (KRT5 − P63 +) (Fig. 3E-F; (E) $F_{3,\ 17} = 0.5$, $p = 0.7$, (F) $H_3 = 0.9$, $p = 0.8$) or superficial (KRT5-P63-) (Fig. 3G-H; (G) $W_{3,\ 7.6} = 0.2$, $p = 0.9$, (H) $F_{3,\ 17} = 1.5$, $p = 0.2$). While we cannot comment on the lineage of these cells, these data do indicate that urothelial composition is not disrupted by developmental PCB exposure. Further, expression of uroplakin III, a product of differentiated superficial cells which contributes to barrier function (Georgas et al., 2015; Khandelwal et al., 2009), was observed in all PCB dose groups, indicative of normal bladder urothelial composition (Supplementary Fig. 1).

3.3. Developmental PCB exposure increases bladder volume in male but not female mice

We next examined whether PCBs have an impact on bladder morphology by measuring bladder volume, changes to which are evident in several genetic and pharmacological rodent models of lower urinary tract dysfunction (Nicholson et al., 2018, 2012; Birder et al., 2002; Grogafe et al., 2009; Singh et al., 2007). Developmental PCB exposure significantly increased bladder volume relative to body mass in male mice in the 6 mg/kg dose group versus vehicle control (Fig. 4A; F3,

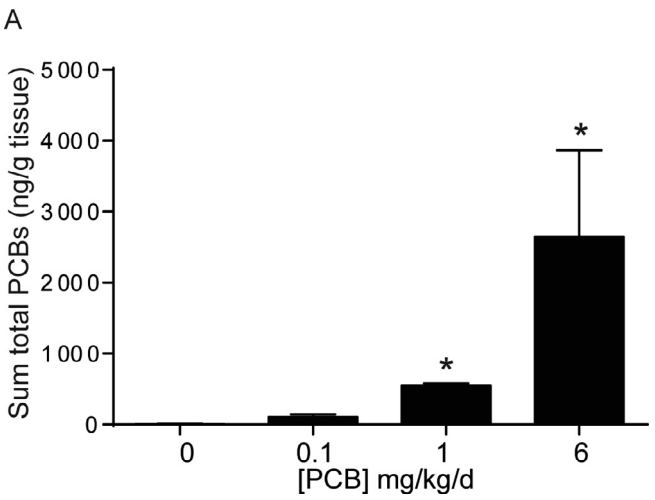

Fig. 1. PCBs are detected in bladder tissue from developmentally exposed offspring. (A) Mice were exposed to PCBs via the maternal diet throughout gestation and lactation. PCB concentrations were measured in bladder tissue from male offspring at postnatal day (P) 28–31. Results are mean ± SEM sum of the total PCB congeners which were detected in at least one sample, n = 3–4 pools of bladder tissue per dose group. For samples where the congener was not detected above the limit of detection, one half of the LOD value was assigned. *Significantly different from vehicle control as determined using Kruskal-Wallis test followed by Dunn's multiple comparisons test, $p \leq 0.05$.

73 = 3.1, p = 0.03). No changes were observed in female mice (Fig. 4B; $F_{3, 21} = 0.8$, p = 0.5). Obstruction can lead to increases in bladder volume (Nicholson et al., 2012; Austin et al., 2004). We therefore examined whether evidence of obstruction was present in PCB exposed bladders. During the course of obstruction, the bladder can undergo an initial phase of compensation, marked by increased bladder mass (Nicholson et al., 2012). However, developmental PCB exposure did not alter bladder mass normalized to body mass (Fig. 4C-D; (C) $F_{3, 88} = 2.2$, p = 0.09, (D) $F_{3, 28} = 0.5$, p = 0.7). In prolonged or severe obstruction, following the compensation phase, the bladder undergoes decompensation, which is marked by thinning of the epithelium (Nicholson et al., 2012). To examine whether there was evidence of bladder decompensation we quantified the thickness of the basal and superficial epithelial layers as indicated by KRT5 and Keratin 20 (KRT20) positive cells, respectively (Fig. 5A-B). PCBs did not alter the thickness of either of these layers, nor the total epithelial thickness in male or female bladders (Fig. 5C–H; (C) $H_3 = 2.3$, p = 0.5, (D) $F_{3, 17} = 0.4$, p = 0.8, (E) $H_3 = 1.7$, p = 0.6, (F) $F_{3, 17} = 1.4$, p = 0.3, (G) $H_3 = 3.3$, p = 0.3, (H) $F_{3, 17} = 0.6$, p = 0.6). Finally, we examined bladder muscle thickness as an indicator of either compensation, which could be marked by increased bladder wall thickness, or decompensation, which could be marked by a decrease in bladder muscle thickness. There were no significant differences in bladder muscle thickness in male or female mice developmentally exposed to PCBs (Supplementary Fig. 2; (B) $F_{3, 18} = 0.9$, p = 0.5, (C) $F_{3, 18} = 0.5$, p = 0.7). These results indicate that PCB-induced changes in male bladder volume occur in the absence of changes to bladder mass, epithelial or muscle thickness, and suggest that obstruction is not likely a key factor.

We also confirmed that PCBs do not cause overt toxicity that could result in changes in normal kidney function thereby altering urine production and bladder volume. Developmental PCB exposure did not significantly alter urinary creatinine or protein in male or female offspring (Supplementary Fig. 3; (A) $F_{3, 21} = 1$, p = 0.4, (B) $F_{3, 13} = 0.8$, p = 0.5, (C) $F_{3, 17} = 2.7$, p = 0.08, (D) $W_{3, 6} = 0.3$, p = 0.9), consistent with normal kidney function. There were also no indications that developmental PCB exposure resulted in an overall developmental delay in mice, as PCB exposure did not significantly change male or female body mass (Supplementary Fig. 4; (A) $F_{3, 96} = 1.8$, p = 0.2, (B) $H_3 = 0.7$, p = 0.9).

3.4. Developmental PCB exposure increases nerve fiber density in a sex- and dose-specific manner in the bladder

We next examined whether histological changes were evident that might contribute to/result from increased bladder volume observed with developmental PCB exposure. Bladder innervation is important in regulating sensory information about bladder fullness and can contribute to changes in volume or sensitivity to filling in mouse models of stress (Mingin et al., 2015), inflammation (Schnegelsberg et al., 2010) and aging (Daly et al., 2014). While decreased nerve density is often observed in obstruction models (Hughes et al., 2019), increased nerve density is prevalent in patients with neurogenic detrusor overactivity and increased afferent nerve fibers are linked to incontinence in women with idiopathic detrusor overactivity (Smet et al., 1997; de Groat and Yoshimura, 2009; Fowler et al., 2008). Since PCBs are also known to alter neuronal morphology in the central nervous system (Wayman et al., 2012b), we examined total βIII-tubulin positive nerve fibers (Coelho et al., 2017) as an indicator of overall nerve density in bladder (Fig. 6A-B). There was a significant increase in the density of nerve fibers expressing βIII-tubulin within 10 μm of the epithelium in male bladders of the 6 mg/kg PCB group versus vehicle control and versus 0.1 mg/kg PCB group (Fig. 6C; $F_{3, 18} = 4.5$, p = 0.02). There were no significant changes in female bladders (Fig. 6D; $F_{3, 18} = 0.5$, p = 0.7). When examining the entire stromal area, data approached, but did not reach, significance, for an increase in the density of nerve fibers expressing βIII-tubulin in male 6 mg/kg dose group versus 0.1 mg/kg dose group (overall one-way ANOVA $F_{3, 18} = 2.7$, p = 0.08, and Tukey's multiple comparisons test between 6 mg/kg and 0.1 mg/kg groups had an adjusted p value of 0.05) (Fig. 6E). There were no differences in stromal area in female bladders (Fig. 6F; $F_{3, 18} = 0.8$, p = 0.5). We next examined the muscle layer. There were no changes in the density of nerve fibers expressing βIII-tubulin in muscle of male or female bladders (Fig. 6G-H; (G) $F_{3, 18} = 1.4$, p = 0.3, (H) $F_{3, 18} = 0.8$, p = 0.5). Overall, effects of PCBs on nerve fiber density tend to be concentrated in the suburothelial layer within 10 μm of the epithelium, a region that is especially important in sensory function and in regulating voiding dynamics (de Groat and Yoshimura, 2009; Birder and de Groat, 2007).

Since the suburothelium was the major site of PCB effects on nerve density, and this region is especially rich in sensory axons (de Groat and Yoshimura, 2009), we chose to examine the sensory component of PCB-induced increases in total nerve density. We determined whether PCBs specifically influence peptidergic sensory afferent axons based on calcitonin gene-related peptide (CGRP) expression (Fig. 7A-B). There was a significant increase in the percentage of CGRP-positive nerve fibers within 10 μm of the epithelium in bladders of males in the 6 mg/kg versus the 0.1 mg/kg PCB group (Fig. 7C; $H_3 = 7.8$, p = 0.05). There were no group differences in female bladders (Fig. 7D; $F_{3, 18} = 0.7$, p = 0.5). Similar to βIII-tubulin, the data approached, but did not reach, significance for an increase in CGRP expression within the total stroma (overall one-way ANOVA $F_{3, 18} = 2.7$, p = 0.08 and Tukey's multiple comparisons test between 6 mg/kg and 0.1 mg/kg groups had an adjusted p value of 0.06) (Fig. 7E). There were no differences in female bladders (Fig. 7F; $F_{3, 18} = 0.7$, p = 0.6). Overall, these results indicate peptidergic sensory nerves are increased in bladder suburothelium of the highest versus lowest PCB dose groups and contribute in part to the increased overall βIII-tubulin positive nerve density observed in the suburothelium of male mice that received the highest PCB dose.

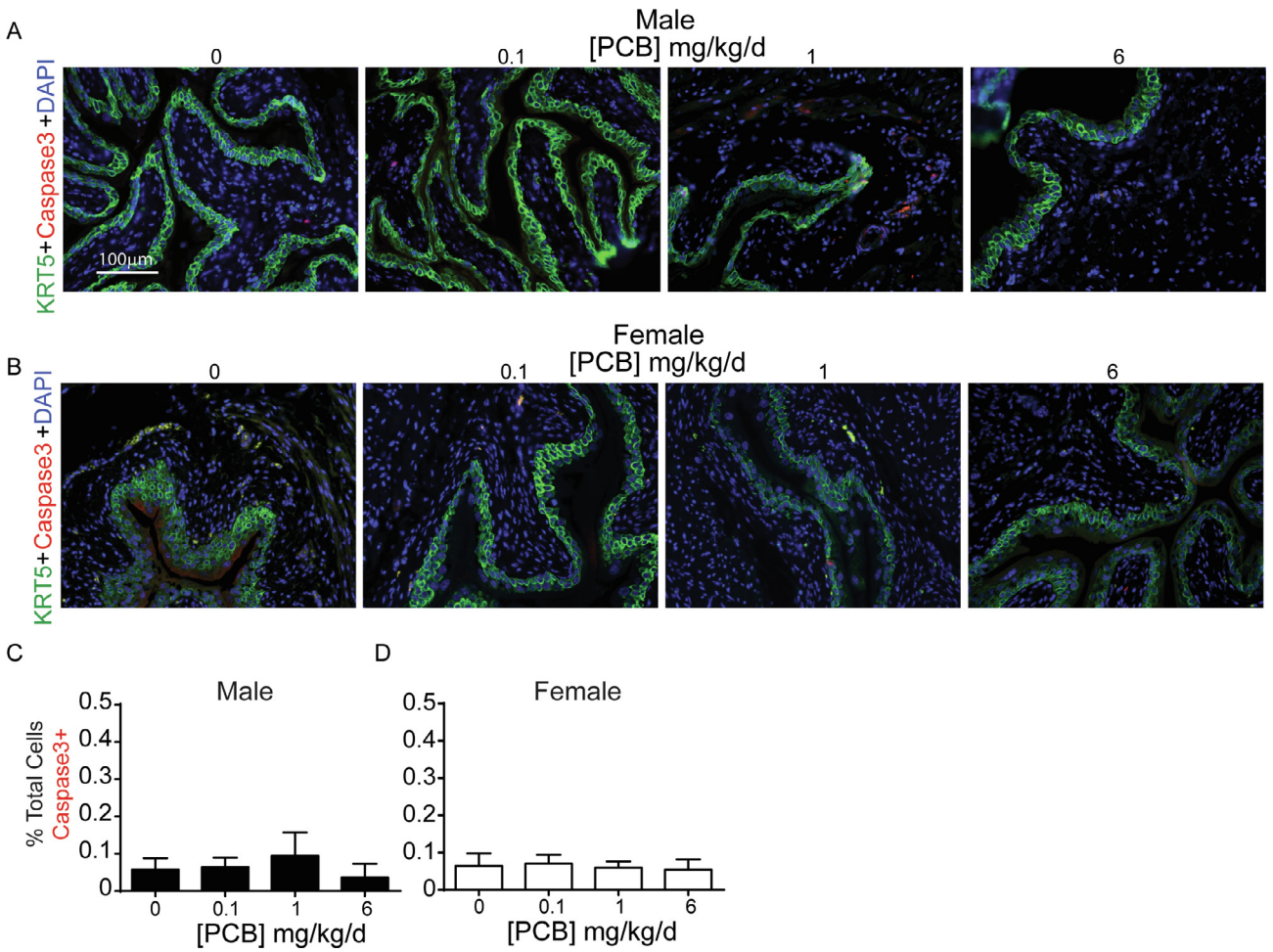

Fig. 2. Developmental PCB exposure does not alter apoptosis in the bladder. Mice were exposed to PCBs via the maternal diet throughout gestation and lactation. Bladders were collected from male and female offspring at postnatal day (P) 28–31 for immunohistochemistry. Representative images of (A) male and (B) female mouse bladders from each PCB dose group incubated with antibodies targeting cleaved caspase 3 (red) to label apoptotic cells, keratin 5 (KRT5, green) to label basal epithelium and DAPI (blue) to stain nuclei. (C-D) Quantification of the percentage of total (stromal and epithelial) cells that were immunopositive for cleaved caspase-3. Results are mean ± SEM, n = 4–6 bladders per group. One-way ANOVA revealed no significant differences. (For interpretation of the references to colour in this figure legend, the reader is referred to the web version of this article.)

3.5. Developmental PCB exposure increases mast cells in a sex- and dose-specific manner in the bladder

Increased bladder nerve density or afferent activity are often observed in animal models of inflammation (Schnegelsberg et al., 2010; Gonzalez et al., 2016; Saban et al., 2011; Vizzard, 2001). To determine whether local inflammation may contribute to PCB effects on nerve density, we examined the number of mast cells within the bladder. Mast cells are often associated with innervation in several tissues including the bladder (Keith et al., 1995), and they are of particular interest in the bladder as inflammatory mediators implicated in disease states, including interstitial cystitis (Kleij and Bienenstock, 2005; Bauer and Razin, 2000; Letourneau et al., 1996; Sant et al., 2007). PCBs have also been linked to activation of mast cell lines (Lauriano et al., 2012; Narita et al., 2007). Therefore, we determined whether PCBs alter mast cell numbers within the bladder. Since PCB changes in nerve density occurred in the lowest and highest concentrations of PCBs, we focused on these groups. There was a significant increase in the total number of mast cells in the bladders in the 6 mg/kg versus the 0.1 mg/kg PCB group in male but not female bladders (Fig. 8A-D; (C) $F_{2, 13} = 3.8$, $p = 0.05$, (D) $F_{2, 13} = 1.8$, $p = 0.2$). We next differentiated between mast cells that were not yet degranulated versus those that were degranulated (Fig. 8F, H insets). There were no significant differences in the number of non-degranulated mast cells (Fig. 8E-F; (E) $H_2 = 5.5$, $p = 0.06$, (F) $F_{2, 13} = 1.2$, $p = 0.3$); however, there was a significant increase in the number of degranulated mast cells in the 6 mg/kg versus the 0.1 mg/kg PCB dose group in male but not female bladders (Fig. 8G-H; (G) $F_{2, 13} = 4.1$, $p = 0.04$, (H) $F_{2, 13} = 1$, $p = 0.4$).

There was a significant positive correlation between total mast cell density and suburothelial βIII-tubulin positive nerve density in the bladders among 0.1 mg/kg and 6 mg/kg PCB samples from combined male and female samples (Fig. 9A). When the sexes were separated, there was a significant positive correlation between total mast cell density and suburothelial βIII-tubulin positive nerve density in male but not female bladders (Fig. 9B). When analyzed within each dose group, there was a significant positive correlation between total mast cell density and suburothelial βIII-tubulin positive nerve density in the 6 mg/kg PCB dose group only (Fig. 9C). These results indicate a positive correlation in mast cells and nerve density within the male bladders that was driven by developmental exposure to PCBs at 6 mg/kg.

4. Discussion

To our knowledge, this is the first preclinical evidence that suggests developmental exposure to PCBs has effects on the bladder. Develop-

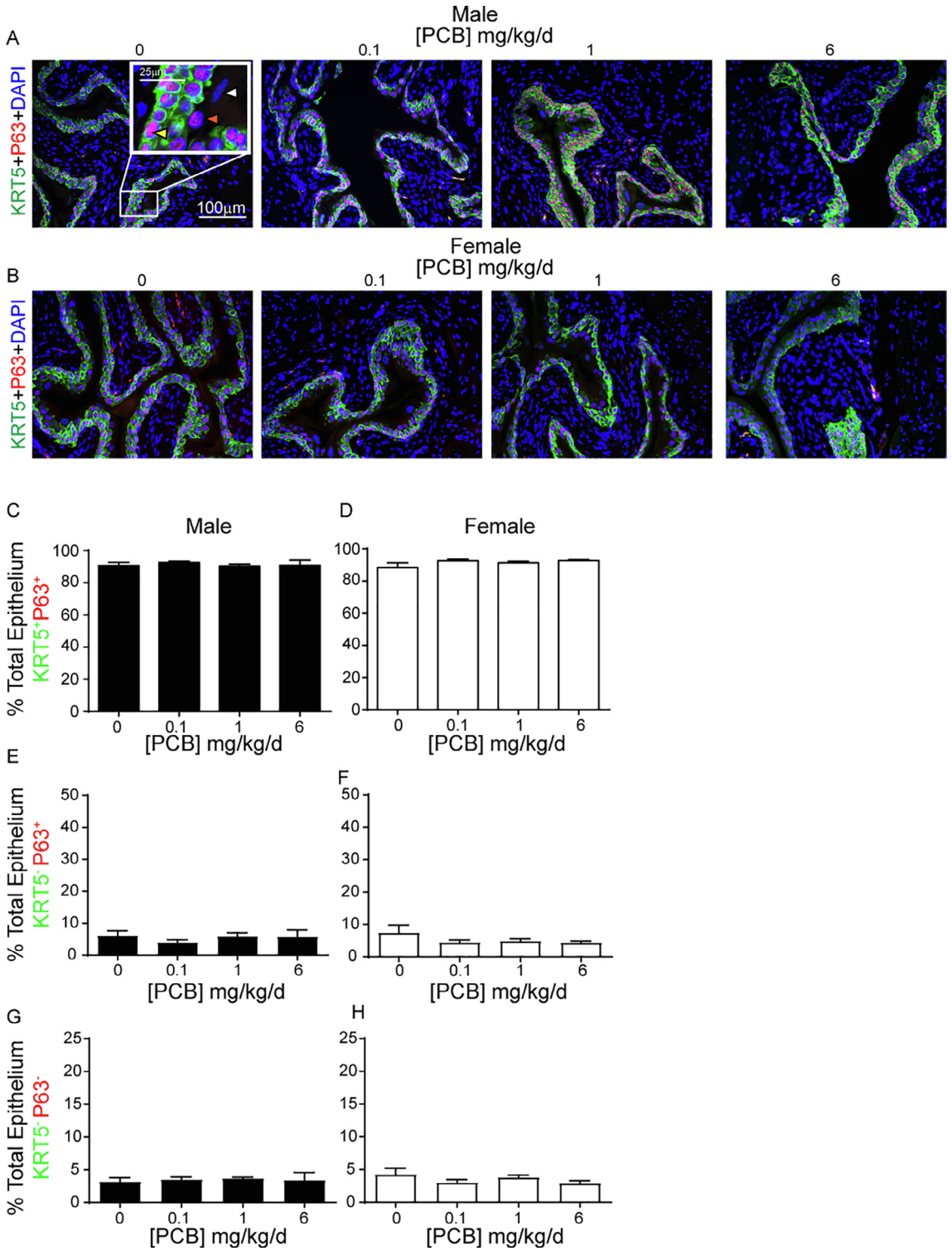

Fig. 3. PCBs do not alter bladder epithelial cell composition in developmentally exposed mice. Mice were exposed to PCBs via the maternal diet throughout gestation and lactation and bladders collected from male and female offspring at postnatal day (P) 28–31 for immunohistochemistry. Representative images of (A) male and (B) female mouse bladders from each PCB dose group incubated with antibodies targeting keratin 5 (KRT5, green) to label basal epithelium, transformation related protein 63 (P63, red) to label basal + intermediate epithelium and DAPI (blue) to stain nuclei. Inset illustrates a cell of each type; basal indicated by the yellow arrowhead, intermediate indicated by the orange arrowhead, and superficial indicated by the white arrowhead. Quantification of the percentage of total epithelial cells that express (C-D) both KRT5 and P63 (basal), (E-F) P63 alone (intermediate), or (G-H) neither KRT5 nor P63 (superficial). Results are mean ± SEM, n = 4–6 bladders per group. (C, E, H) One-way ANOVA or (D, G) Welch's one-way ANOVA or (F) Kruskal-Wallis tests revealed no significant differences. (For interpretation of the references to colour in this figure legend, the reader is referred to the web version of this article.)

mental exposure of mice to PCBs not only results in dose-dependent levels of PCBs detectable within bladder tissue, but also increases bladder volume and suburothelial total nerve density in male mice of the 6 mg/kg vs control group. Increases in nerve density are coincident with increases in mast cells, suggesting that inflammatory mediators may play a role in PCB-induced effects on the bladder. Together, these

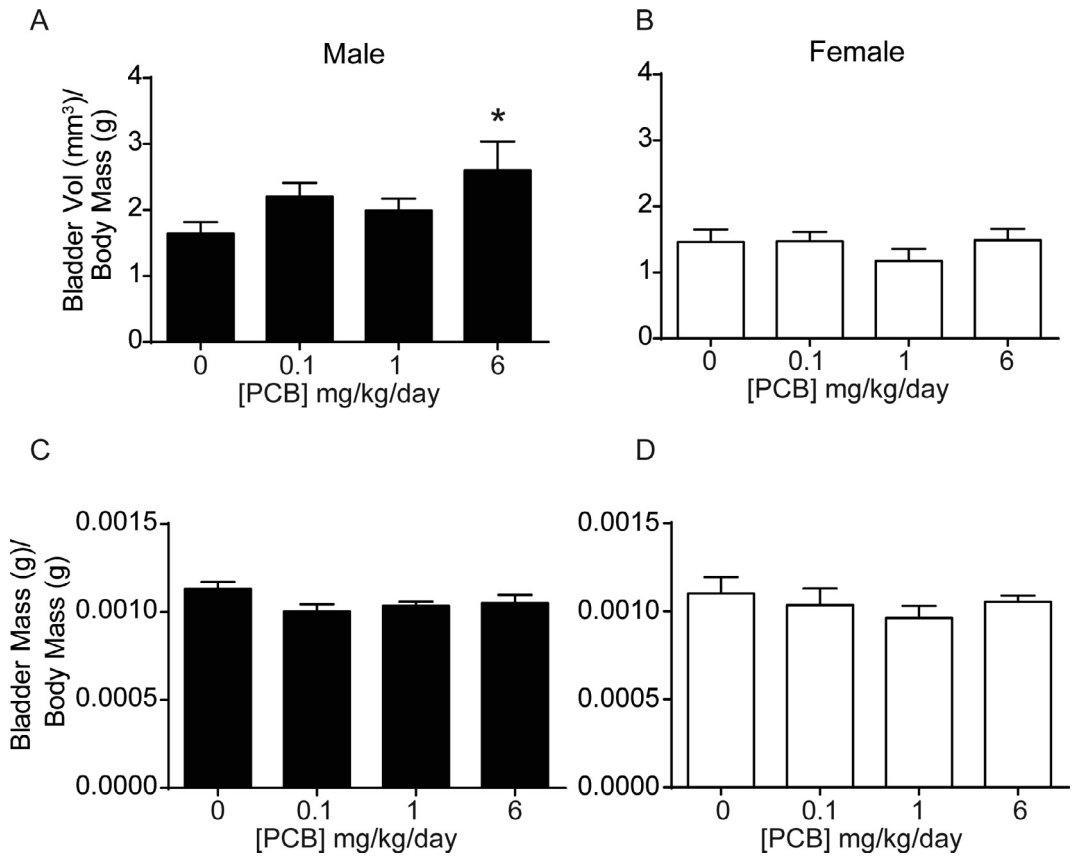

Fig. 4. PCBs increase bladder volume in developmentally exposed male but not female mice. Mice were exposed to PCBs via the maternal diet throughout gestation and lactation and bladder metrics measured in male and female offspring at postnatal day (P) 28–31. (A-B) Bladder volume normalized to body mass, (C-D) Bladder mass normalized to body mass. Results are mean ± SEM, n values for vehicle control, 0.1, 1.0, and 6.0 mg/kg/d PCB dose groups, respectively, were (A-B) Males n = 20,23,18,16; Females 4,7,8,6; (C-D) Males n = 22,26,27,17; Females 4,10,8,10. Samples were obtained from 6 to 8 litters for male and 3–4 litters for female. *Significantly different from same sex vehicle control as determined by one-way ANOVA with Tukey's multiple comparisons tests, $p \leq 0.05$. A mixed effects model to control for litter (nested one-way ANOVA in Prism) revealed the same statistical differences.

results suggest PCBs modulate bladder function. Whether these changes persist, alter voiding dynamics, or enhance the effect of other stressors later in life is unknown but readily testable.

Our results suggest that gestational and lactational exposure to the environmentally relevant MARBLES PCB mixture used here, leads to detectable levels of PCBs in bladder tissue of exposed male offspring 7–10 days after the last possible lactational exposure, and results in an increase in total tissue PCB concentration at the 1 mg/kg and 6 mg/kg PCB dose groups compared to vehicle control. This dose-dependent increase is consistent with other rodent PCB dosing studies using Aroclor PCB mixtures or single congeners such as PCB 95 (Yang et al., 2009; Kania-Korwel et al., 2015). The dose-dependent increase in PCB tissue concentration does not follow a linear relationship with the dose administered to the dam. This is also observed in other studies, (Kania-Korwel et al., 2012, 2008) and the non-linear relationship may be in part due to dose-dependent effects on cytochrome P450 metabolizing enzyme induction (Kania-Korwel et al., 2012). It can be difficult to compare tissue concentrations of PCB across studies due to differences in species studied, PCB congeners analyzed, dosing mixtures, dosing paradigms, and/or extraction or normalization methods. However, the dosing paradigm used here results in a range of PCB concentrations in developmentally exposed offspring mouse bladders that recapitulates the spectrum of sum total concentrations found in the environment in tissue from fish (Ashley et al., 2009) to birds (Levengood and Schaeffer, 2010) to humans (Li et al., 2019; Jacobson et al., 1990). There are also similarities in single congeners. Of the more abundant congeners examined in human breast tissue on a ng/g wet weight basis, maximum concentrations for PCB 138 (120 ng/g), 153 (145 ng/g) and 180 (84 ng/g) were between the values reported here for those congeners in the 1 and 6 mg/kg PCB groups (Li et al., 2019). Overall, these data suggest that the dosing paradigm used here results in bladder PCB concentrations in weanling mice that are environmentally relevant, recapitulating the low and high ends of the spectrum of PCBs found in biological samples.

PCBs vary in organ distribution, and where the bladder falls in terms of total tissue burden of PCBs relative to other organs is unknown. While we did not directly compare the whole bladder tissue to muscle, liver, or adipose in our study, examining PCB concentrations across tissues in the same animal would greatly help us to understand where bladder falls in the spectrum of PCB tissue body burdens. This could be of further benefit if bladder concentrations correlate with other more commonly sampled tissues, making it possible to predict bladder PCB burden in humans.

The bladder is also a unique target organ in that it not only has a tissue compartment to which PCBs can distribute from the systemic circulation, but also functions to store urine that contains PCBs and their metabolites. Human data indicate that PCBs are not only detected in urine, but concentrations of PCB 52, PCB 28 and PCB 101 can be higher in urine compared to blood (urine/blood ratio of 1.6, 1.2, and 1.6 respectively) (Genuis et al., 2013). While the bladder is efficient in its barrier function to eliminate toxins within the urine, the contribution of urinary PCBs to the total bladder tissue PCB burden is unknown. It is especially relevant to examine whether disease conditions such as diabetes, infection or inflammation – which may

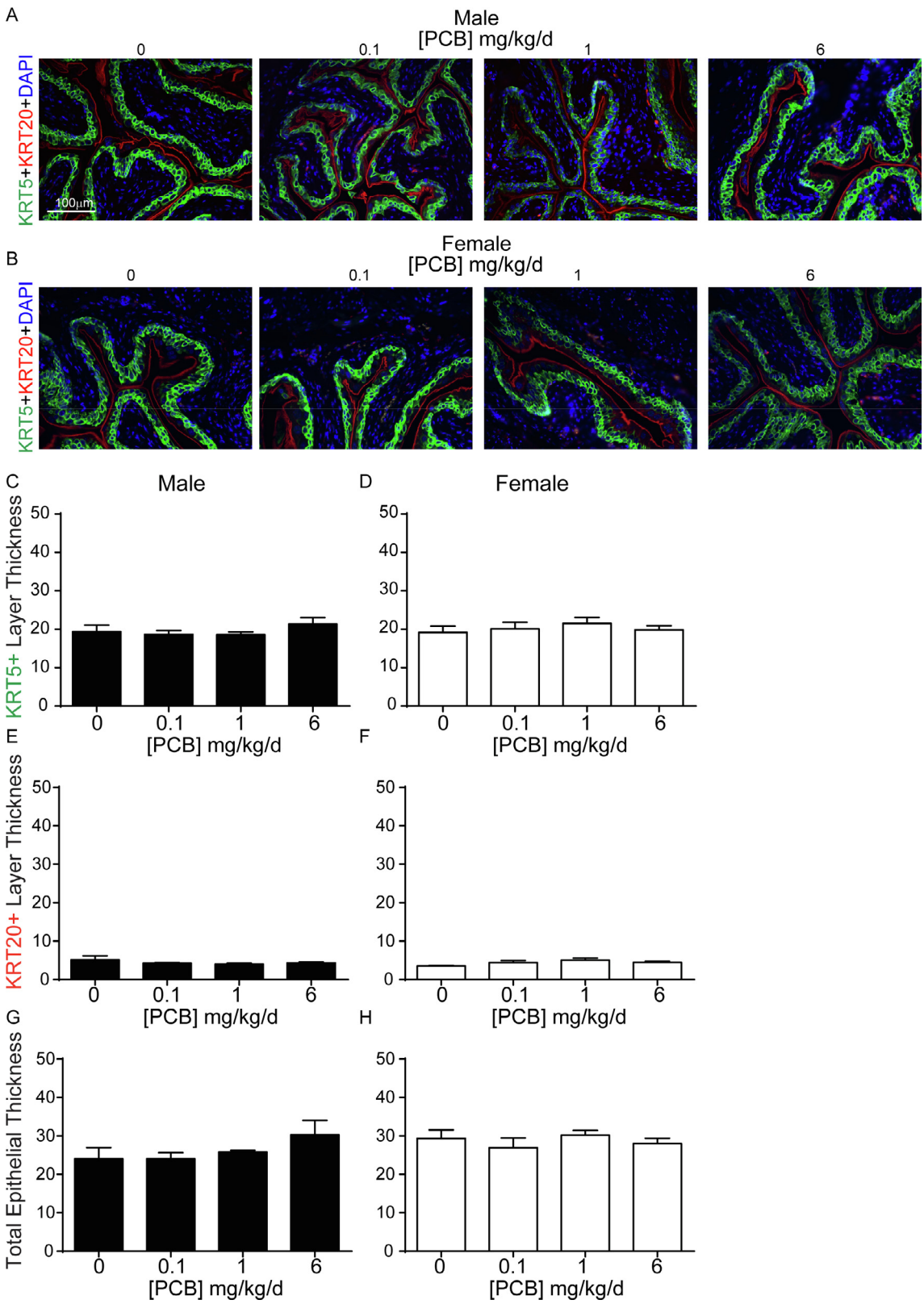

Fig. 5. PCBs do not alter bladder epithelial cell thickness in developmentally exposed mice. Mice were exposed to PCBs via the maternal diet throughout gestation and lactation and bladders collected from male and female offspring at postnatal day (P) 28–31 for immunohistochemistry. Representative images of (A) male and (B) female mouse bladders from each PCB exposure group incubated with antibodies targeting keratin 5 (KRT5, green) to label basal epithelium, keratin 20 (KRT20, red) to label superficial epithelium and DAPI (blue) to stain nuclei. Quantification of epithelial thickness (microns) of cells that express (C-D) KRT5, (E-F) KRT20, or (G-H) total epithelium KRT5 + KRT20 layers. Results are mean ± SEM, n = 3–6 bladders per group. (D, F, H) One-way ANOVA or (C, E, G) Kruskal-Wallis test revealed no significant differences. (For interpretation of the references to colour in this figure legend, the reader is referred to the web version of this article.)

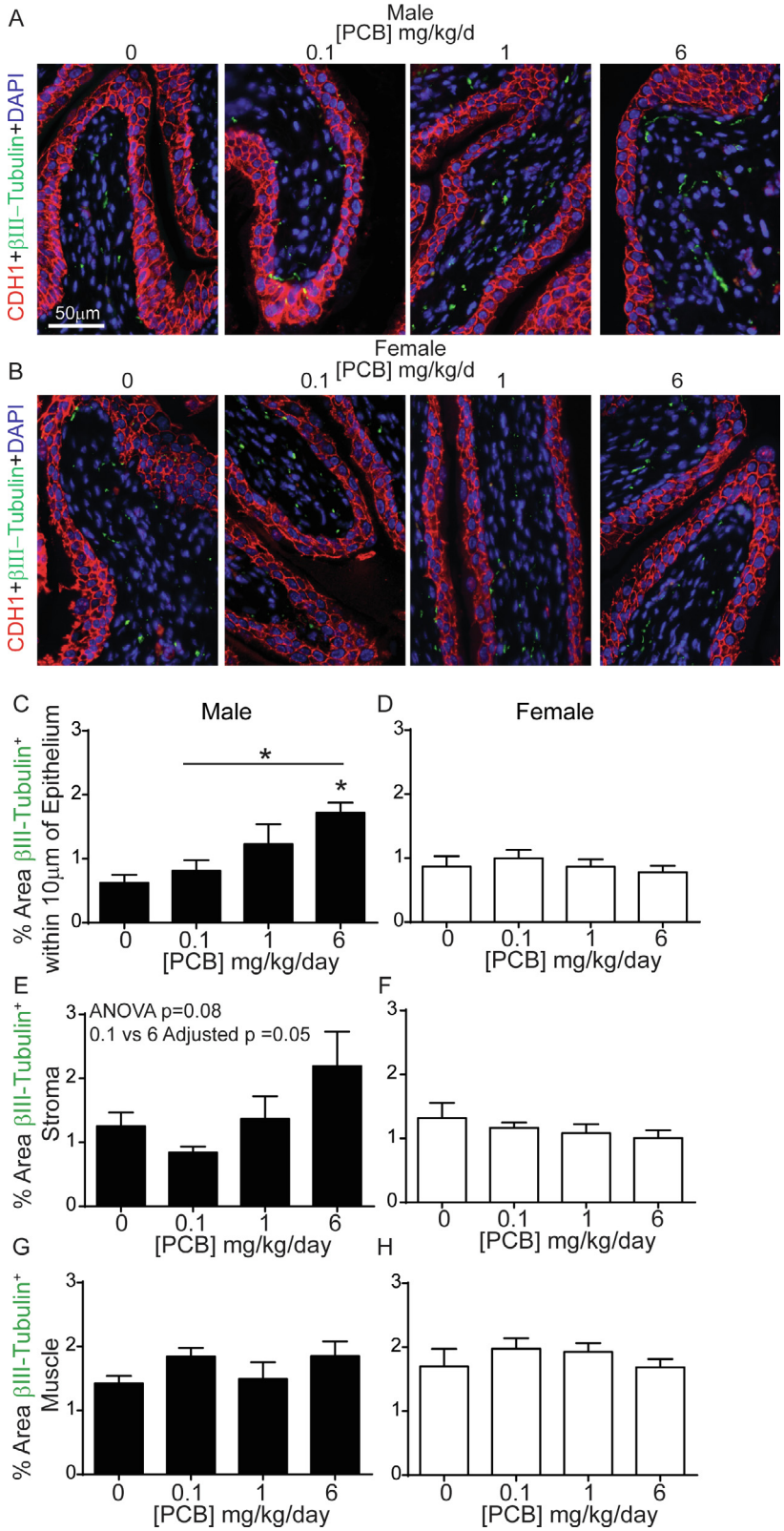

Fig. 6. PCBs increase βIII-tubulin positive nerve fibers in bladder of developmentally exposed mice. Mice were exposed to PCBs via the maternal diet throughout gestation and lactation and bladders collected from male and female offspring at postnatal day (P) 28–31 for immunohistochemistry. Representative images of (A) male and (B) female mouse bladders (epithelium and stroma) from each PCB dose group incubated with antibodies targeting beta III tubulin (β-tubulin, green) to label nerve fibers, e-cadherin (CDH1, red) to label all epithelium and DAPI (blue) to stain nuclei. Quantification of (C-D) the percent area within 10 μm of the epithelium with βIII-tubulin positive nerve fibers, (E-F) percent area of stroma with βIII-tubulin positive nerve fibers, (G-H) percent area of muscle with βIII-tubulin positive nerve fibers. Results are mean ± SEM, n = 4–6 bladders per group. *Significantly different versus same sex vehicle control, bar and * indicate other significant differences as determined using one-way ANOVA followed by Tukey's multiple comparisons tests, $p \leq 0.05$. (For interpretation of the references to colour in this figure legend, the reader is referred to the web version of this article.)

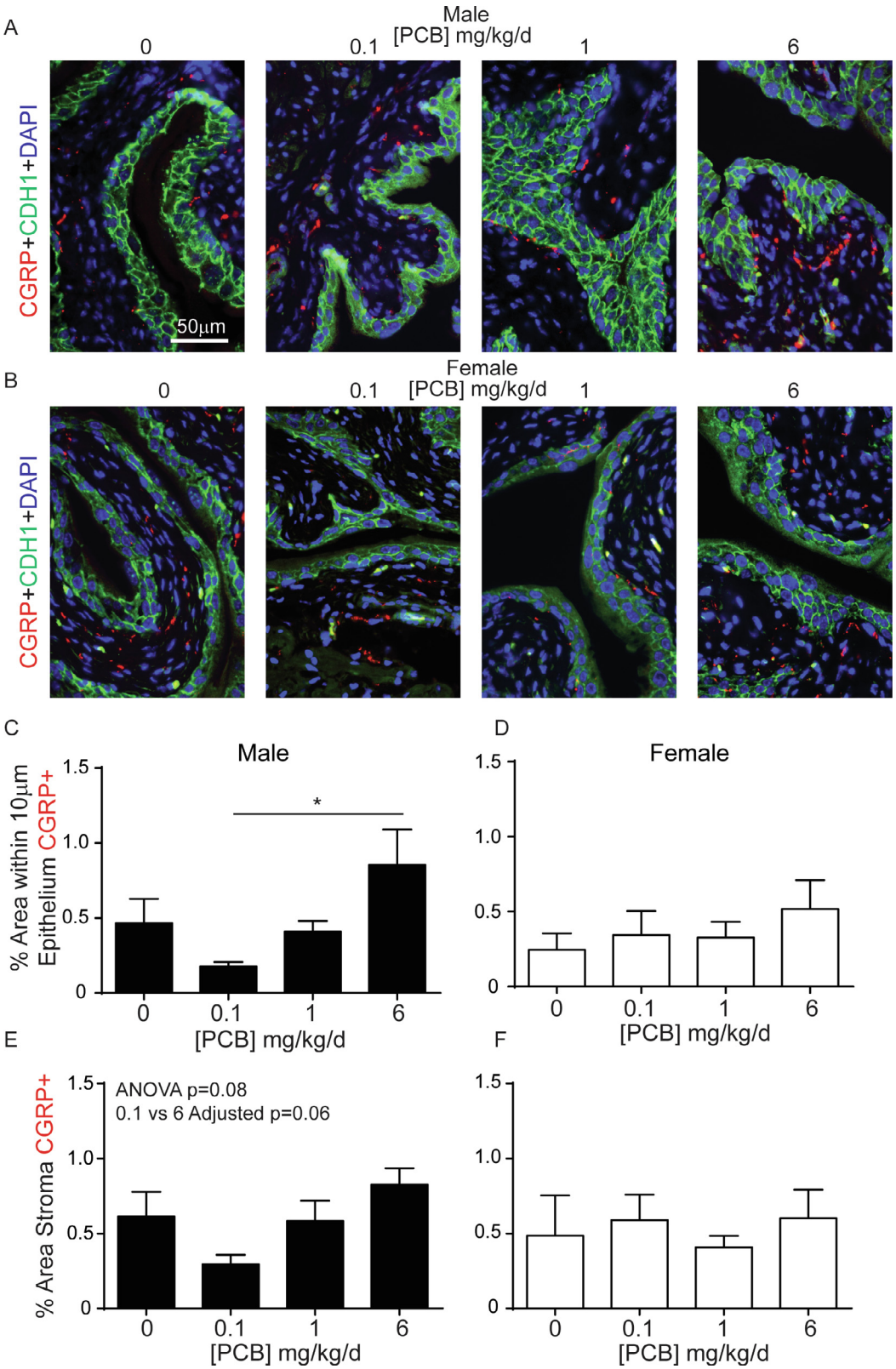

Fig. 7. Increased CGRP-positive nerve fibers in bladder of mice developmentally exposed to PCBs at 6 mg/kg vs 0.1 mg/kg. Mice were exposed to PCBs via the maternal diet throughout gestation and lactation and bladders collected from male and female offspring at postnatal day (P) 28–31 for immunohistochemistry. Representative images of (A) male and (B) female mouse bladders from each PCB dose group incubated with antibodies targeting calcitonin gene-related peptide (CGRP, red) to label afferent sensory nerve fibers, e-cadherin (CDH1, green) to label all epithelium and DAPI (blue) to stain nuclei. Quantification of (C-D) the percent area within 10 µm of the epithelium with CGRP-positive nerve fibers, (E-F) percent area stroma with CGRP-positive nerve fibers. Results are mean ± SEM, n = 4–6 bladders per group. (D, E, F) One-way ANOVA or (C) Kruskal-Wallis test were used to determine significant differences. (C) Bar and * indicate significant differences as determined using Kruskal-Wallis test followed by Dunn's multiple comparisons tests, $p < 0.05$. (For interpretation of the references to colour in this figure legend, the reader is referred to the web version of this article.)

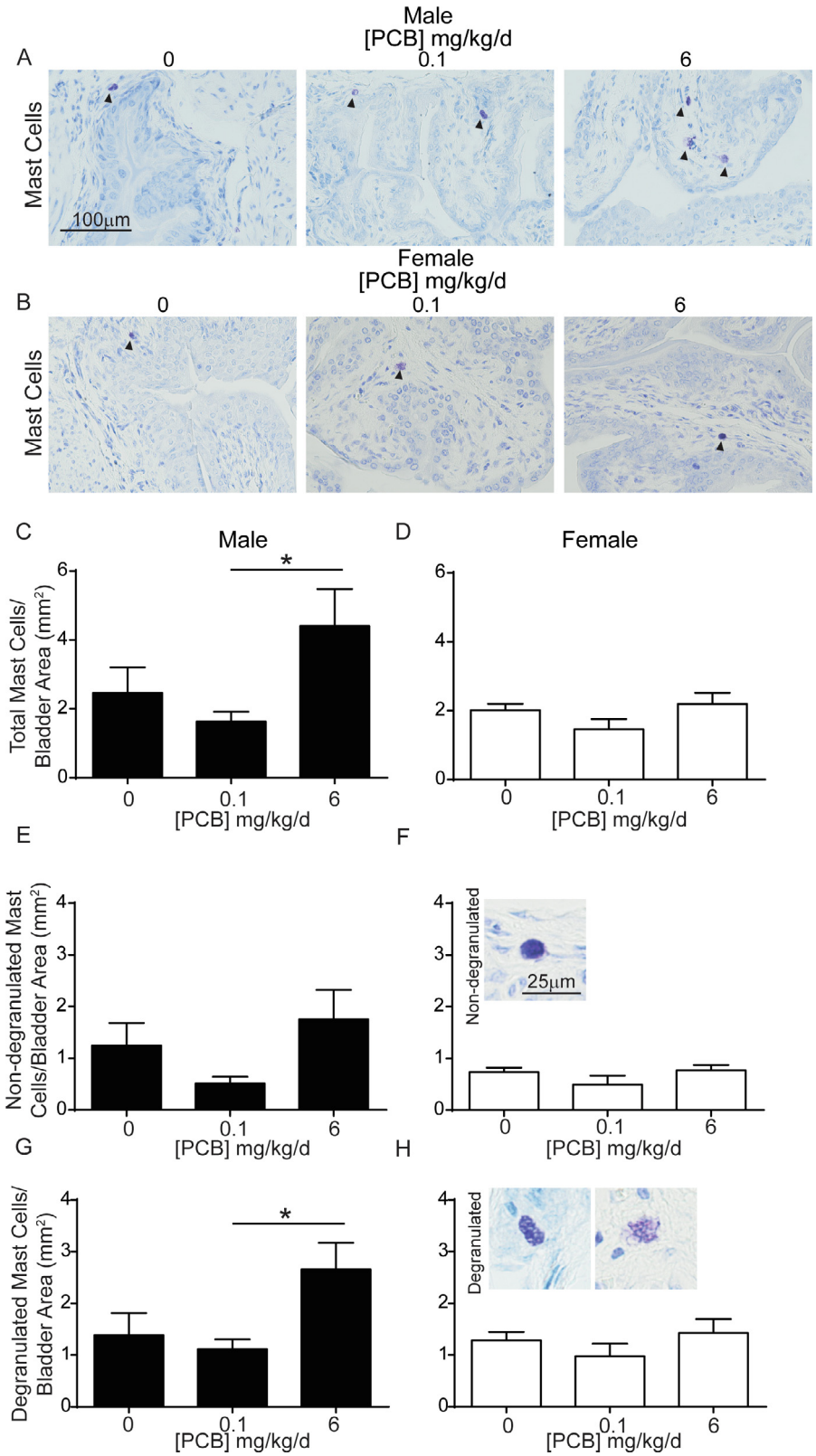

Fig. 8. Increased mast cells in bladder of mice developmentally exposed to PCBs at 6 mg/kg vs 0.1 mg/kg. Mice were exposed to PCBs via the maternal diet throughout gestation and lactation and bladders collected from male and female offspring at postnatal day (P) 28–31. Representative images of (A) male and (B) female mouse bladders from each PCB dose group stained with toluidine blue to identify mast cells (purple). Quantification of (C-D) total number of mast cells normalized to bladder area, (E-F) non-degranulated mast cells normalized to bladder area, (G-H) degranulated mast cells normalized to bladder area. Results are mean ± SEM, n = 4–6 bladders per group. (C, D, F-H) One-way ANOVA or (E) Kruskal-Wallis test were used to determine significant differences. Bar and * indicate significant differences as determined using one-way ANOVA followed by Tukey's multiple comparisons tests, $p \leq 0.05$. (For interpretation of the references to colour in this figure legend, the reader is referred to the web version of this article.)

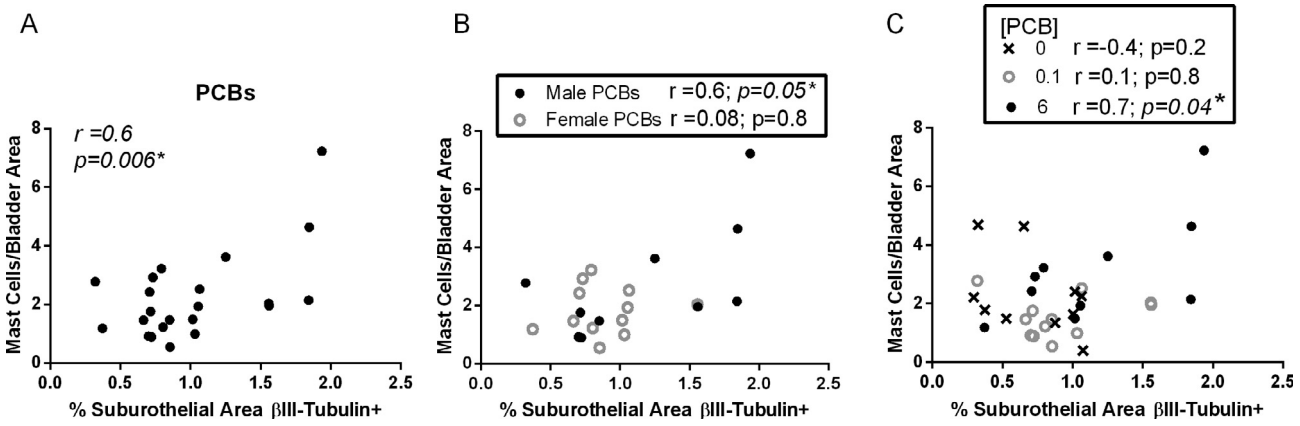

Fig. 9. βIII-tubulin positive nerve fiber density and mast cells are positively correlated in PCB exposed bladders. Mice were exposed to PCBs via the maternal diet throughout gestation and lactation and bladders collected from male and female offspring at postnatal day (P) 28–31. Correlation between the percentage area of suburothelium βIII-tubulin positive versus total mast cells/bladder area for each sample. (A) Both sexes of 0.1 mg/kg and 6 mg/kg PCB groups were combined, n = 22 samples. (B) For each sex independently, 0.1 mg/kg and 6 mg/kg PCB groups were combined to determine a correlation, n = 10 male PCB samples; n = 12 female PCB samples. (C) Both sexes were combined from each group separately to determine a correlation, n = 10 control samples, n = 12 PCB 0.1 mg/kg/d, n = 10 PCB 6 mg/kg/d. * indicates significance determined by Pearson r at $p \leq 0.05$.

compromise the bladder's barrier function – lead to increased bladder tissue burden of PCBs from the urine and in turn contribute to increased risk of bladder dysfunction. While we did not observe PCB effects on apoptosis of bladder epithelial cells, we cannot rule out the possibility that PCBs trigger necrosis within bladder epithelium as we did not examine this endpoint. Future studies to address this possibility could provide insight on whether PCBs can alter barrier function.

One of the observed phenotypes in our study was an increase in bladder volume in PCB-exposed male mice. There are several possible mechanisms which may contribute to this phenotype. One possible mechanism leading to this phenotype is bladder outlet/urethral obstruction (Nicholson et al., 2012; Austin et al., 2004). For example, in the testosterone and estradiol (T + E2) aging mouse obstruction model, a severe increase in bladder volume accompanied by a thinning, decompensated bladder, is observed in adult mice after 2–4 months of hormone treatment (Nicholson et al., 2012). However, in contrast to this model, male mice in the 6 mg/kg PCB dose group did not have an increase in bladder mass or changes to epithelial or muscle thickness – endpoints that would suggest remodeling of the bladder wall or decompensation of the bladder as a result of severe or prolonged obstruction (Nicholson et al., 2012). Together, these results indicate that at the time point examined, obstruction is not likely a key driver of PCB-induced changes in male bladder volume. Other interpretations include the possibility that the bladder may have a greater capacity to hold urine but not to the extent that the bladder remodels. This may be a phenomenon of the time point examined, and it is possible that later in life, bladder mass and epithelial thickness would change, indicative of bladder wall remodeling as a result of prolonged increased bladder volume.

Another possible mechanism that may underlie PCB-induced increases in bladder volume are changes in neural control of micturition. Bladder innervation is essential to voiding function, and changes to nerve density and/or sensory function are commonly observed in patients with LUTS (Smet et al., 1997; Radziszewski et al., 2009). Typically, decreased nerve density is seen in rodent obstruction models with enlarged bladders (Hughes et al., 2019). Here too, our results are not suggestive of an obstruction model, as we did not observe a decrease in nerve density, rather, we saw a PCB-induced increase in nerve density in males of the 6 mg/kg PCB group compared to sex-matched vehicle controls. The observation of increased nerve density may be functionally linked to increased bladder volume. The increase in bladder volume may represent an increase in post void residual urine, such that incomplete emptying occurs with each void (Ballstaedt and Woodbury, 2020). Low volume voids or large post void residual are documented in patients who suffer from detrusor overactivity, neurogenic bladder, detrusor-sphincter dyssynergia and infection/cystitis (Ballstaedt and Woodbury, 2020). Patients with spinal cord injury develop hyperexcitability of bladder afferent nerves, which can lead to neurogenic detrusor overactivity or inefficient voiding when bladder and sphincter contraction/relaxation are not coordinated, resulting in detrusor-sphincter dyssynergia (Fowler et al., 2008; Ballstaedt and Woodbury, 2020; Ginsberg, 2013). Collectively, these observations suggest a model in which developmental PCB exposures alter the normal circuitry within the bladder and/or sphincter, leading to abnormal sensation, contractility and/or uncoordinated nerve signaling, which result in inefficient voiding. While we did not test whether there were any changes in nerve activity, this could be done in the future to understand whether PCB-induced changes in nerve density correlate with changes in afferent sensitivity or bladder muscle contractility. A limitation of the common practice of measuring bladder volumes post-euthanasia is that there is no way to determine the status of the bladder prior to measuring. The use of ultrasound or post void residual volume measurements in animals undergoing anesthetized cystometry will be necessary in our model to determine if bladder volumes are altered as a result of post void residual urine secondary to a decrease in voiding efficiency.

In the current study, we cannot rule out the possibility that PCB-induced changes in bladder volume are mediated by increases in water intake. However, several lines of evidence suggest this is not likely a major contributor. Other studies have found that while PCB exposure can prevent a rise in central vasopressin (Coburn et al., 2007, 2005) – this is only observed in a state of dehydration (Coburn et al., 2005). Further in this same study, basal water intake in rats did not differ upon treatment with Aroclor 1254 (Coburn et al., 2005). In our study, concentrations of urinary creatinine and protein were unaltered. While it is possible that absolute levels of creatinine and protein in the urine may be higher based on no change in concentration and increased bladder volume, this effect remains to be determined. On the other hand, if animals were producing a more dilute urine, we would expect to see a decrease in urinary creatinine and protein concentration. For example, in a rat model of fluid homeostasis, treatment with an FGF21 analog results in a 20% increase in water intake, increased urine output and a decrease in urine electrolytes and creatinine (Turner et al., 2018). In our study, we did not observe PCB effects on body mass, so if food or water consumption did increase with PCB exposure, it

was not to a level that altered body mass. Future studies to examine water intake, vasopressin release, urine osmolality and renal function will be useful to assess impacts of developmental PCB exposure on fluid balance.

PCB effects on bladder volume may also be mediated by a behavioral mechanism. Increased bladder volumes are observed in rodent models of stress. Different stressors can result in increased voiding volume (fewer, larger voids) (Chang et al., 2009) or increased micturition frequency of smaller volumes (Mingin et al., 2015, 2014; Tykocki et al., 2018). Thus the type, severity and duration of stress contribute to the spectrum of either urine retention (underactivity) or overactive bladder phenotypes (Mingin et al., 2014). It is also interesting to note that stress-induced changes in bladder capacity are not always accompanied by changes in bladder mass (Mingin et al., 2014), which is consistent with our observations of male mice developmentally exposed to PCBs. Further, models of stress-induced bladder dysfunction can result in changes to bladder sensory nerve activity (Mingin et al., 2015). For example, stress increased *ex vivo* bladder volume and afferent activity recorded from the pelvic nerve in mice (Mingin et al., 2015). While we did not measure nerve activity, we did observe increased nerve fiber density in the suburothelium and increased bladder volume in response to developmental PCBs. We also observed an increase in CGRP positive nerves in bladder suburothelium in males of the 6 mg/kg versus 0.1 mg/kg PCB groups. CGRP nerves are linked to stress-induced changes in bladder function (Mingin et al., 2015). In mouse models of stress, expression of the transient receptor potential cation channel subfamily V member 1 (TRPV1) within CGRP positive neurons is elevated, suggesting an increase in sensory afferents (Mingin et al., 2015). Pharmacological inhibition of TRPV1 channels decreases afferent activity and overactive voiding parameters (Mingin et al., 2015). Whether our mixture of PCBs increases stress, alters afferent nerve activity, or alters TRPV1 expression is unknown, but PCBs have been linked to decreased performance on rodent learning and memory tasks (Yang et al., 2009) as well as increased anxious behavior (Elnar et al., 2012). Increased stress may explain effects on the bladder observed here and may also manifest in changes to voiding function which are an avenue of future study. Stress related bladder dysfunction is a major contributor to decreased quality of life and identifying modifiable risk factors in the environment that could help to identify individuals at risk or provide more effective targeted therapies to improve bladder control are necessary.

PCBs are known to induce inflammatory responses in other tissues (Rude et al., 2019; Bell et al., 2018; Petriello et al., 2018a, 2018b) and changes in nerve density and increased afferent sensitivity are observed in states of bladder inflammation (de Groat and Yoshimura, 2009). Thus, it is possible that the increase in nerve density we observed in the bladder is in part mediated by an inflammatory response at some point in time. This is also supported by the finding of increased number of mast cells in the bladder of 6 mg/kg PCB dose group compared to the 0.1 mg/kg dose group. This is of interest because mast cells can serve as a link between the immune and nervous system both in health and disease (Kleij and Bienenstock, 2005; Letourneau et al., 1996). Many tissues, including the bladder, exhibit mast cells and nerves in close proximity (Keith et al., 1995; Kleij and Bienenstock, 2005; Bauer and Razin, 2000). This is especially true in patients with interstitial cystitis (Sant et al., 2007; Ratliff et al., 1995). PCBs have been linked to increases in mast cells in intestine of fish (Lauriano et al., 2012), and PCBs have been shown to induce degranulation in mast cell lines through mechanisms involving estrogen receptor alpha (Narita et al., 2007). This is especially interesting since PCB 28 is a major constituent of the mixture used here and has been shown to have estrogenic activity (Plíšková et al., 2005). Whether the observed changes in mast cells observed here are elicited by estrogenic actions of PCBs is an area of future study. Further, whether PCB-induced increases in mast cells and nerve density contribute to changes in voiding function are unknown but this possibility is of clinical significance because several LUTS such as painful bladder syndrome/interstitial cystitis and overactive bladder exhibit abnormal sensory signaling and inflammation.

The ability of environmental chemicals, especially during development, to impact urinary function throughout life is an area of increasing interest (Ricke et al., 2016; Taylor et al., 2020; Turco et al., 2020). Others have found links between 2,3,7,8-tetrachlorodibenzodioxin (dioxin or TCDD) and impaired lower urinary tract function (Ricke et al., 2016; Turco et al., 2020). This is of interest given that a subset of PCBs are structurally similar to dioxin and the PCB mixture used here contains PCB 118 (at 4.9% of mix), which is a dioxin-like PCB. Developmental dioxin exposure in mice later challenged with T + E2 hormones to mimic male aging, exacerbates hormone effects on bladder mass and collagen density (Ricke et al., 2016), and in wild type mice increases urine spot number in the void spot assay (Turco et al., 2020). Additional studies of developmental dioxin exposure and lower urinary tract function found differential prostate proteomic profiles with dioxin + T + E2 vs T + E2 alone (Turco et al., 2020). Of particular interest was the finding that ryanodine receptor 1 was upregulated in dioxin T + E2 compared to T + E2 treatment alone (Turco et al., 2020). The non-dioxin-like PCBs, which make up the majority of our PCB mixture, are known to increase dendritic complexity via sensitization of ryanodine receptors in the central nervous system (Wayman et al., 2012b). The role of ryanodine receptor in PCB effects in the bladder are unknown but readily testable. Further this raises the intriguing hypothesis that dioxin-like PCBs may in turn make the lower urinary tract more susceptible to non-dioxin-like PCBs via upregulation of ryanodine receptor. Understanding the individual effects of each MARBLES PCB congener on morphology and function are warranted for informing the risk posed by environmental PCBs for LUTS.

Sex differences were observed for many of the endpoints altered by PCBs. This is consistent with other studies that found sex-dependent effects of PCBs in rodent liver (Wahlang et al., 2019), bone (Romero et al., 2017), cultured neurons (Keil et al., 2018; Sethi et al., 2017b) and in serum cytokine levels in response to immune challenge (Bell et al., 2018). PCB body burdens differ between male and female fish samples, with males generally having higher concentrations than females (Madenjian et al., 2015, 2016, 2017). We did not examine PCB levels in male compared to female bladder and thus cannot rule out differences in PCB body burden between the sexes, this is an area of future study. However, this possibility is not likely a large contributing factor. Other studies have reported that there are no sex differences in PCB congener content in the entire carcass of P3 and P7 offspring or in the blood, brain, liver and muscle of P21 offspring in studies which used a similar dosing paradigm to the one used here (Kania-Korwel et al., 2017). Other rodent studies using Aroclor PCB mixture, A1254, in a similar dosing paradigm to the one used here also observed no sex differences in brain PCB content in P62 offspring (Dziennis et al., 2008). In addition to PCB-induced changes in steroid hormones and signaling pathways, sex differences in response to PCB exposure could also be a result of effects of sex hormones/chromosomes on sexually differentiated targets which leads to differential sensitivity to PCBs. Another mechanism leading to sex differences in response to PCBs could be in PCB metabolism, as was found with hydroxylated PCB 136 in liver slices, in part due to differential expression of cytochrome P450 enzymes (Wu et al., 2013; Kato and Yamazoe, 1992). Since some PCB metabolites have been shown to have similar or in some cases even more severe adverse effects on cells or neurons *in vitro* (Sethi et al., 2019, 2017c), examining the distribution of PCB metabolites in the bladder as well as any sex-dependent changes in metabolism or disposition is an area of future study which will help us to better understand underlying mechanisms of PCB exposure on bladder morphology and function.

Bladder function is a major factor in quality of life. Evidence that bladder dysfunction is a common comorbidity in patients diagnosed

with neurodevelopmental disorders (von Gontard et al., 2011; von Gontard et al., 2015) coupled with evidence that PCBs may enhance neurodevelopmental disorder risk (Lyall et al., 2017; Schantz et al., 2003; Pessah et al., 2019) make it plausible that PCBs alone may contribute to lower urinary tract function. Understanding whether and how a modifiable risk factor like PCB exposure contributes to bladder dysfunction in health and disease could greatly improve therapeutic strategies to prevent, identify and treat patients with bladder dysfunction.

Funding

This work was supported by the United States National Institutes of Health grants [R00 ES029537 to KPKS, R01 ES014901, P01 ES011269, and P30 ES023513 to PJL, T32 ES007059 to SS, and T32 ES007015 to CLK]; and the United States Environmental Protection Agency grant [R833292 to PJL]. This project used core facilities supported by the MIND Institute Intellectual and Developmental Disabilities Research Center grant [U54 HD079125], the National Institutes of Health National Center for Advancing Translational Sciences grant [UL1 TR000002], the University of Wisconsin O'Brien Center for Benign Urologic Research grant [U54 DK104310 to DEB] and the Superfund Research Center at The University of Iowa grant [P42 ES013661]. The content is solely the responsibility of the authors and does not necessarily represent the official views of the NIH or the USEPA. Further, the NIH and USEPA did not endorse the purchase of any commercial products or services mentioned in the publication.

CRediT authorship contribution statement

Kimberly P. Keil Stietz: Conceptualization, Methodology, Validation, Formal analysis, Investigation, Visualization, Writing - original draft, Writing - review & editing, Supervision, Funding acquisition. **Conner L. Kennedy:** Methodology, Validation, Investigation, Visualization, Writing - original draft, Writing - review & editing. **Sunjay Sethi:** Methodology, Validation, Investigation, Writing - review & editing. **Anthony Valenzuela:** Methodology, Validation, Investigation, Writing - review & editing. **Alexandra Nunez:** Validation, Investigation, Writing - original draft, Writing - review & editing. **Kathy Wang:** Validation, Investigation, Writing - original draft, Writing - review & editing. **Zunyi Wang:** Validation, Investigation, Writing - review & editing. **Peiqing Wang:** Validation, Investigation, Writing - review & editing. **Audrey Spiegelhoff:** Validation, Visualization, Writing - review & editing. **Birgit Puschner:** Supervision, Methodology, Writing - review & editing, Funding acquisition. **Dale E. Bjorling:** Supervision, Methodology, Writing - review & editing, Funding acquisition. **Pamela J. Lein:** Supervision, Methodology, Writing - review & editing, Funding acquisition.

Declaration of Competing Interest

The authors declare that they have no known competing financial interests or personal relationships that could have appeared to influence the work reported in this paper.

Acknowledgements

We would like to acknowledge Dr. Xueshu Li and Dr. Hans-Jaochim Lehmler from the University of Iowa for the synthesis of the PCBs used in this study and Dr. Ingrid Gennity (University of California, Davis) for her assistance in method development for the PCB analysis.

Conflict of Interest

The authors have no conflicts of interest to declare.

Appendix A. Supplementary data

Supplementary data to this article can be found online at https://doi.org/10.1016/j.crtox.2021.01.002.

Reference

Abler, L.L., Keil, K.P., Mehta, V., Joshi, P.S., Schmitz, C.T., Vezina, C.M., 2011. A high-resolution molecular atlas of the fetal mouse lower urogenital tract. Dev. Dyn. 240, 2364–2377. https://doi.org/10.1002/dvdy.22730.

Ampleman, M.D., Martinez, A., DeWall, J., Rawn, D.F.K., Hornbuckle, K.C., Thorne, P.S., 2015. Inhalation and dietary exposure to pcbs in urban and rural cohorts via congener-specific measurements. Environ. Sci. Technol. 49, 1156–1164. https://doi.org/10.1021/es5048039.

Arms, L., Vizzard, M.A., 2011. Neuropeptides in lower urinary tract function. Handb. Exp. Pharmacol.. https://doi.org/10.1007/978-3-642-16499-6_19. 10.1007/978-3-642-16499-6_19, 395-423.

Ashley, J.T.F., Webster, M.L., Horwitz, R.J., Velinsky, D.J., Baker, J.E., 2009. Polychlorinated biphenyls in sediment and biota from the Delaware river estuary. Proc. Acad. Nat. Sci. Philadelphia 158, 89–105.

Austin, J.C., Chacko, S.K., DiSanto, M., Canning, D.A., Zderic, S.A., 2004. A male murine model of partial bladder outlet obstruction reveals changes in detrusor morphology, contractility and Myosin isoform expression. J. Urol. 172, 1524–1528.

Ballstaedt, L., Woodbury, B., 2020. Bladder Post Void Residual Volume. StatPearls, Treasure Island (FL).

Barmpas, M., Vakonaki, E., Tzatzarakis, M., Sifakis, S., Alegakis, A., Grigoriadis, T., Sodré, D.B., Daskalakis, G., Antsaklis, A., Tsatsakis, A., 2020. Organochlorine pollutants' levels in hair, amniotic fluid and serum samples of pregnant women in Greece: A cohort study. Environ. Toxicol. Pharmacol. 73, 103279. https://doi.org/10.1016/j.etap.2019.103279.

Bauer, O., Razin, E., 2000. Mast cell-nerve interactions. Physiology 15, 213–218. https://doi.org/10.1152/physiologyonline.2000.15.5.213.

Bell, M.R., Dryden, A., Will, R., Gore, A.C., 2018. Sex differences in effects of gestational polychlorinated biphenyl exposure on hypothalamic neuroimmune and neuromodulator systems in neonatal rats. Toxicol. Appl. Pharmacol. 353, 55–66. https://doi.org/10.1016/j.taap.2018.06.002.

Birder, L.A., de Groat, W.C., 2007. Mechanisms of disease: involvement of the urothelium in bladder dysfunction. Nat. Rev. Urol. 4, 46–54. https://doi.org/10.1038/ncpuro0672.

Birder, L.A., Nakamura, Y., Kiss, S., Nealen, M.L., Barrick, S., Kanai, A.J., Wang, E., Ruiz, G., de Groat, W.C., Apodaca, G., Watkins, S., Caterina, M.J., 2002. Altered urinary bladder function in mice lacking the vanilloid receptor TRPV1. Nat. Neurosci. 5, 856–860. https://doi.org/10.1038/nn902.

Chang, A., Butler, S., Sliwoski, J., Valentino, R., Canning, D., Zderic, S., 2009. Social stress in mice induces voiding dysfunction and bladder wall remodeling. Am. J. Physiol. Renal Physiol. 297, F1101–F1108. https://doi.org/10.1152/ajprenal.90749.2008.

Chen, X., Lin, Y., Dang, K., Puschner, B., 2017. Quantification of polychlorinated biphenyls and polybrominated diphenyl ethers in commercial cows' milk from California by gas chromatography-triple quadruple mass spectrometry. PloS One 12,. https://doi.org/10.1371/journal.pone.0170129 e0170129.

Chu, S., Covaci, A., Schepens, P., 2003. Levels and chiral signatures of persistent organochlorine pollutants in human tissues from Belgium. Environ. Res. 93, 167–176.

Coburn, C.G., Gillard, E.R., Curras-Collazo, M.C., 2005. Dietary exposure to aroclor 1254 alters central and peripheral vasopressin release in response to dehydration in the rat. Toxicol. Sci. 84, 149–156. https://doi.org/10.1093/toxsci/kfi046.

Coburn, C.G., Curras-Collazo, M.C., Kodavanti, P.R., 2007. Polybrominated diphenyl ethers and ortho-substituted polychlorinated biphenyls as neuroendocrine disruptors of vasopressin release: effects during physiological activation in vitro and structure-activity relationships. Toxicol. Sci. 98, 178–186. https://doi.org/10.1093/toxsci/kfm086.

Cockayne, D.A., Dunn, P.M., Zhong, Y., Rong, W., Hamilton, S.G., Knight, G.E., Ruan, H. Z., Ma, B., Yip, P., Nunn, P., et al, 2005. P2X2 knockout mice and P2X2/P2X3 double knockout mice reveal a role for the P2X2 receptor subunit in mediating multiple sensory effects of ATP. J. Physiol. 567, 621–639. https://doi.org/10.1113/jphysiol.2005.088435.

Coelho, A., Antunes-Lopes, T., Gillespie, J., Cruz, F., 2017. Beta-3 adrenergic receptor is expressed in acetylcholine-containing nerve fibers of the human urinary bladder: an immunohistochemical study. Neurourol. Urodyn. 36, 1972–1980. https://doi.org/10.1002/nau.23224.

Covaci, A., de Boer, J., Ryan, J.J., Voorspoels, S., Schepens, P., 2002. Distribution of organobrominated and organochlorinated contaminants in Belgian human adipose tissue. Environ. Res. 88, 210–218. https://doi.org/10.1006/enrs.2002.4334.

Daly, D.M., Nocchi, L., Liaskos, M., McKay, N.G., Chapple, C., Grundy, D., 2014. Age-related changes in afferent pathways and urothelial function in the male mouse bladder. J. Physiol. 592, 537–549. https://doi.org/10.1113/jphysiol.2013.262634.

de Groat, W.C., Yoshimura, N., 2009. Afferent nerve regulation of bladder function in health and disease. Handb. Exp. Pharmacol., 91–138. https://doi.org/10.1007/978-3-540-79090-7_4. 10.1007/978-3-540-79090-7_4, 91-138.

Dewailly, E., Mulvad, G., Pedersen, H.S., Ayotte, P., Demers, A., Weber, J.P., Hansen, J. C., 1999. Concentration of organochlorines in human brain, liver, and adipose tissue autopsy samples from Greenland. Environ. Health Perspect. 107, 823–828.

Dziennis, S., Yang, D., Cheng, J., Anderson, K.A., Alkayed, N.J., Hurn, P.D., Lein, P.J., 2008. Developmental exposure to polychlorinated biphenyls influences stroke outcome in adult rats. Environ. Health Perspect. 116, 474–480. https://doi.org/10.1289/ehp.10828.

Elnar, A.A., Diesel, B., Desor, F., Feidt, C., Bouayed, J., Kiemer, A.K., Soulimani, R., 2012. Neurodevelopmental and behavioral toxicity via lactational exposure to the sum of six indicator non-dioxin-like-polychlorinated biphenyls (summation operator6 NDL-PCBs) in mice. Toxicology 299, 44–54. https://doi.org/10.1016/j.tox.2012.05.004.

Eubig, P.A., Aguiar, A., Schantz, S.L., 2010. Lead and PCBs as risk factors for attention deficit/hyperactivity disorder. Environ. Health Perspect. 118, 1654–1667. https://doi.org/10.1289/ehp.0901852.

Fowler, C.J., Griffiths, D., de Groat, W.C., 2008. The neural control of micturition. Nat. Rev. Neurosci. 9, 453–466. https://doi.org/10.1038/nrn2401.

Gandhi, D., Molotkov, A., Batourina, E., Schneider, K., Dan, H., Reiley, M., Laufer, E., Metzger, D., Liang, F., Liao, Y., et al, 2013. Retinoid signaling in progenitors controls specification and regeneration of the urothelium. Dev. Cell 26, 469–482. https://doi.org/10.1016/j.devcel.2013.07.017.

Genuis, S.J., Beesoon, S., Birkholz, D., 2013. Biomonitoring and elimination of perfluorinated compounds and polychlorinated biphenyls through perspiration: blood, urine, and sweat study. ISRN Toxicol. 2013, 1–7. https://doi.org/10.1155/2013/483832.

Georgas, K.M., Armstrong, J., Keast, J.R., Larkins, C.E., McHugh, K.M., Southard-Smith, E.M., Cohn, M.J., Batourina, E., Dan, H., Schneider, K., Buehler, D.P., Wiese, C.B., Brennan, J., Davies, J.A., Harding, S.D., Baldock, R.A., Little, M.H., Vezina, C.M., Mendelsohn, C., 2015. An illustrated anatomical ontology of the developing mouse lower urogenital tract. Development 142, 1893–1908. https://doi.org/10.1242/dev.117903.

Ghosh, S., De, S., Chen, Y., Sutton, D.C., Ayorinde, F.O., Dutta, S.K., 2010. Polychlorinated biphenyls (PCB-153) and (PCB-77) absorption in human liver (HepG2) and kidney (HK2) cells in vitro: PCB levels and cell death. Environ. Int. 36, 893–900. https://doi.org/10.1016/j.envint.2010.06.010.

Ginsberg, D., 2013. The epidemiology and pathophysiology of neurogenic bladder. Am. J. Manage. Care 19, s191–196.

Gografe, S.I., Sanberg, P.R., Chamizo, W., Monforte, H., Garbuzova-Davis, S., 2009. Novel pathologic findings associated with urinary retention in a mouse model of mucopolysaccharidosis type IIIB. Comp. Med. 59, 139–146.

Gonzalez, E.J., Heppner, T.J., Nelson, M.T., Vizzard, M.A., 2016. Purinergic signalling underlies transforming growth factor-beta-mediated bladder afferent nerve hyperexcitability. J. Physiol. 594, 3575–3588. https://doi.org/10.1113/JP272148.

Granillo, L., Sethi, S., Keil, K.P., Lin, Y., Ozonoff, S., Iosif, A.M., Puschner, B., Schmidt, R. J., 2019. Polychlorinated biphenyls influence on autism spectrum disorder risk in the MARBLES cohort. Environ. Res. 171, 177–184. https://doi.org/10.1016/j.envres.2018.12.061.

Gubbiotti, M., Elisei, S., Bedetti, C., Marchiafava, M., Giannantoni, A., 2019a. Urinary and bowel disfunction in autism spectrum disorder: a prospective, observational study. Psychiatr. Danub. 31, 475–478.

Gubbiotti, M., Balboni, G., Bini, V., Elisei, S., Bedetti, C., Marchiafava, M., Giannantoni, A., 2019b. Bladder and bowel dysfunction, adaptive behaviour and psychiatric profiles in adults affected by autism spectrum disorders. Neurourol. Urodyn. 38, 1866–1873. https://doi.org/10.1002/nau.24081.

Hertz-Picciotto, I., Schmidt, R.J., Walker, C.K., Bennett, D.H., Oliver, M., Shedd-Wise, K. M., LaSalle, J.M., Giulivi, C., Puschner, B., Thomas, J., Roa, D.L., Pessah, I.N., Van de Water, J., Tancredi, D.J., Ozonoff, S., 2018. A Prospective study of environmental exposures and early biomarkers in autism spectrum disorder: design, protocols, and preliminary data from the MARBLES study. Environ. Health Perspect. 126,. https://doi.org/10.1289/EHP535 117004.

Hu, D., Hornbuckle, K.C., 2010. Inadvertent polychlorinated biphenyls in commercial paint pigments. Environ. Sci. Technol. 44, 2822–2827. https://doi.org/10.1021/es902413k.

Hughes Jr., F.M., Sexton, S.J., Ledig, P.D., Yun, C.E., Jin, H., Purves, J.T., 2019. Bladder decompensation and reduction in nerve density in a rat model of chronic bladder outlet obstruction are attenuated with the NLRP3 inhibitor glyburide. Am. J. Physiol. Renal Physiol. 316, F113–F120. https://doi.org/10.1152/ajprenal.00400.2018.

Jacobson, J.L., Jacobson, S.W., Humphrey, H.E.B., 1990. Effects of in utero exposure to polychlorinated biphenyls and related contaminants on cognitive functioning in young children. J. Pediatr. 116, 38–45. https://doi.org/10.1016/s0022-3476(05)81642-7.

Joseph, D.B., Chandrashekar, A.S., Abler, L.L., Chu, L.F., Thomson, J.A., Mendelsohn, C., Vezina, C.M., 2018. In vivo replacement of damaged bladder urothelium by Wolffian duct epithelial cells. Proc. Natl. Acad. Sci. U.S.A. 115, 8394–8399. https://doi.org/10.1073/pnas.1802966115.

Kania-Korwel, I., Hornbuckle, K.C., Robertson, L.W., Lehmler, H.-J., 2008. Dose-dependent enantiomeric enrichment of 2,2',3,3',6,6'-hexachlorobiphenyl in female mice. Environ. Toxicol. Chem. 27, 299. https://doi.org/10.1897/07-359R.1.

Kania-Korwel, I., Barnhart, C.D., Stamou, M., Truong, K.M., El-Komy, M.H.M.E., Lein, P. J., Veng-Pedersen, P., Lehmler, H.-J., 2012. 2,2′,3,5′,6-Pentachlorobiphenyl (PCB 95) and its hydroxylated metabolites are enantiomerically enriched in female mice. Environ. Sci. Technol. 46, 11393–11401. https://doi.org/10.1021/es302810t.

Kania-Korwel, I., Barnhart, C.D., Lein, P.J., Lehmler, H.-J., 2015. Effect of pregnancy on the disposition of 2,2′,3,5′,6-pentachlorobiphenyl (PCB 95) atropisomers and their hydroxylated metabolites in female mice. Chem. Res. Toxicol. 28, 1774–1783. https://doi.org/10.1021/acs.chemrestox.5b00241.

Kania-Korwel, I., Lukasiewicz, T., Barnhart, C.D., Stamou, M., Chung, H., Kelly, K.M., Bandiera, S., Lein, P.J., Lehmler, H.J., 2017. Editor's highlight: congener-specific disposition of chiral polychlorinated biphenyls in lactating mice and their offspring: implications for PCB developmental neurotoxicity. Toxicol. Sci. 158, 101–115. https://doi.org/10.1093/toxsci/kfx071.

Kato, R., Yamazoe, Y., 1992. Sex-specific cytochrome P450 as a cause of sex-and species-related differences in drug toxicity. Toxicol. Lett. 64-65, 661–667. https://doi.org/10.1016/0378-4274(92)90245-f.

Keil, K.P., Sethi, S., Lein, P.J., 2018. Sex-dependent effects of 2,2',3,5',6-pentachlorobiphenyl (PCB 95) on dendritic arborization of primary mouse neurons. Toxicol. Sci.. https://doi.org/10.1093/toxsci/kfy277.

Keil, K.P., Sethi, S., Wilson, M.D., Silverman, J.L., Pessah, I.N., Lein, P.J., 2019. Genetic mutations in Ca 2+ signaling alter dendrite morphology and social approach in juvenile mice. Genes Brain Behav. 18,. https://doi.org/10.1111/gbb.12526 e12526.

Keith, I.M., Jin, J., Saban, R., 1995. Nerve-mast cell interaction in normal guinea pig urinary bladder. J. Comp. Neurol. 363, 28–36. https://doi.org/10.1002/cne.903630104.

Khandelwal, P., Abraham, S.N., Apodaca, G., 2009. Cell biology and physiology of the uroepithelium. Am. J. Physiol. Renal Physiol. 297, F1477–F1501. https://doi.org/10.1152/ajprenal.00327.2009.

Kleij, H., Bienenstock, J., 2005. Significance of conversation between mast cells and nerves. Allergy Asthma Clin. Immunol. 1, 65–80. https://doi.org/10.1186/1710-1492-1-2-65.

Klocke, C., Lein, P.J., 2020. Evidence implicating non-dioxin-like congeners as the key mediators of polychlorinated biphenyl (PCB) developmental neurotoxicity. Int J Mol Sci 21. https://doi.org/10.3390/ijms21031013.

Klocke, C., Sethi, S., Lein, P.J., 2020. The developmental neurotoxicity of legacy vs. contemporary polychlorinated biphenyls (PCBs): similarities and differences. Environ. Sci. Pollut. Res. 27, 8885–8896. https://doi.org/10.1007/s11356-019-06723-5.

Kullmann, F.A., Birder, L.A., Andersson, K.-E., 2015. Translational research and functional changes in voiding function in older adults. Clin. Geriatr. Med. 31, 535–548. https://doi.org/10.1016/j.cger.2015.06.001.

Lauriano, E.R., Calò, M., Silvestri, G., Zaccone, D., Pergolizzi, S., Lo Cascio, P., 2012. Mast cells in the intestine and gills of the sea bream, Sparus aurata, exposed to a polychlorinated biphenyl, PCB 126. Acta Histochem. 114, 166–171. https://doi.org/10.1016/j.acthis.2011.04.004.

Lee, Y.W., Park, H.J., Son, K.W., Hennig, B., Robertson, L.W., Toborek, M., 2003. 2,2′,4,6,6′-Pentachlorobiphenyl (PCB 104) induces apoptosis of human microvascular endothelial cells through the caspase-dependent activation of CREB. Toxicol. Appl. Pharmacol. 189, 1–10. https://doi.org/10.1016/s0041-008x(03)00084-x.

Letourneau, R., Pang, X., Sant, G.R., Theoharides, T.C., 1996. Intragranular activation of bladder mast cells and their association with nerve processes in interstitial cystitis. Br. J. Urol. 77, 41–54. https://doi.org/10.1046/j.1464-410x.1996.08178.x.

Levengood, J.M., Schaeffer, D.J., 2010. Comparison of PCB congener profiles in the embryos and principal prey of a breeding colony of black-crowned night-herons. J. Great Lakes Res. 36, 548–553. https://doi.org/10.1016/j.jglr.2010.04.011.

Li, A.J., Feldman, S.M., McNally, R.K., Kannan, K., 2019. Distribution of organohalogen and synthetic musk compounds in breast adipose tissue of breast cancer patients in Ulster County, New York, USA. Arch. Environ. Contam. Toxicol. 77, 68–78. https://doi.org/10.1007/s00244-019-00621-0.

Lin, Y.P., Pessah, I.N., Puschner, B., 2013. Simultaneous determination of polybrominated diphenyl ethers and polychlorinated biphenyls by gas chromatography-tandem mass spectrometry in human serum and plasma. Talanta 113, 41–48. https://doi.org/10.1016/j.talanta.2013.04.001.

Lyall, K., Croen, L.A., Sjödin, A., Yoshida, C.K., Zerbo, O., Kharrazi, M., Windham, G.C., 2017. Polychlorinated biphenyl and organochlorine pesticide concentrations in maternal mid-pregnancy serum samples: association with autism spectrum disorder and intellectual disability. Environ. Health Perspect. 125, 474–480. https://doi.org/10.1289/EHP277.

Madenjian, C.P., Ebener, M.P., Sepúlveda, M.S., 2015. PCB concentrations of lake Whitefish (Coregonus clupeaformis) vary by sex. J. Great Lakes Res. 41, 1185–1190. https://doi.org/10.1016/j.jglr.2015.09.010.

Madenjian, C.P., Rediske, R.R., Krabbenhoft, D.P., Stapanian, M.A., Chernyak, S.M., O'Keefe, J.P., 2016. Sex differences in contaminant concentrations of fish: a synthesis. Biol. Sex Differ. 7, 42. https://doi.org/10.1186/s13293-016-0090-x.

Madenjian, C.P., Stevens, A.L., Stapanian, M.A., Batterman, S.A., Chernyak, S.M., Menczer, J.E., McIntyre, P.B., 2017. Sex difference in PCB concentrations of a catostomid fish. J. Environ. Anal. Toxicol. 7, 515. https://doi.org/10.4172/2161-0525.1000515.

Marek, R.F., Thorne, P.S., Herkert, N.J., Awad, A.M., Hornbuckle, K.C., 2017. Airborne PCBs and OH-PCBs inside and outside urban and rural U.S. schools. Environ. Sci. Technol. 51, 7853–7860. https://doi.org/10.1021/acs.est.7b01910.

Mingin, G.C., Peterson, A., Erickson, C.S., Nelson, M.T., Vizzard, M.A., 2014. Social stress induces changes in urinary bladder function, bladder NGF content, and generalized bladder inflammation in mice. Am. J. Physiol. Regul. Integr. Comp. Physiol. 307, R893–R900. https://doi.org/10.1152/ajpregu.00500.2013.

Mingin, G.C., Heppner, T.J., Tykocki, N.R., Erickson, C.S., Vizzard, M.A., Nelson, M.T., 2015. Social stress in mice induces urinary bladder overactivity and increases TRPV 1 channel-dependent afferent nerve activity. Am. J. Physiol. Regul. Integr. Comp. Physiol. 309, R629–R638. https://doi.org/10.1152/ajpregu.00013.2015.

Mitchell, M.M., Woods, R., Chi, L.-H., Schmidt, R.J., Pessah, I.N., Kostyniak, P.J., LaSalle, J.M., 2012. Levels of select PCB and PBDE congeners in human postmortem brain reveal possible environmental involvement in 15q11-q13 duplication autism spectrum disorder. Environ. Mol. Mutagen. 53, 589–598. https://doi.org/10.1002/em.21722.

Narita, S., Goldblum, R.M., Watson, C.S., Brooks, E.G., Estes, D.M., Curran, E.M., Midoro-Horiuti, T., 2007. Environmental estrogens induce mast cell degranulation and enhance IgE-mediated release of allergic mediators. Environ. Health Perspect. 115, 48–52. https://doi.org/10.1289/ehp.9378.

Nicholson, T.M., Ricke, E.A., Marker, P.C., Miano, J.M., Mayer, R.D., Timms, B.G., vom Saal, F.S., Wood, R.W., Ricke, W.A., 2012. Testosterone and 17beta-estradiol induce glandular prostatic growth, bladder outlet obstruction, and voiding dysfunction in male mice. Endocrinology 153, 5556–5565. https://doi.org/10.1210/en.2012-1522.

Nicholson, T.M., Nguyen, J.L., Leverson, G.E., Taylor, J.A., vom Saal, F.S., Wood, R.W., Ricke, W.A., 2018. Endocrine disruptor bisphenol A is implicated in urinary voiding dysfunction in male mice. Am. J. Physiol. Renal Physiol. 315, F1208–F1216. https://doi.org/10.1152/ajprenal.00582.2017.

Pessah, I.N., Lein, P.J., Seegal, R.F., Sagiv, S.K., 2019. Neurotoxicity of polychlorinated biphenyls and related organohalogens. Acta Neuropathol. 138, 363–387. https://doi.org/10.1007/s00401-019-01978-1.

Petriello, M.C., Brandon, J.A., Hoffman, J., Wang, C., Tripathi, H., Abdel-Latif, A., Ye, X., Li, X., Yang, L., Lee, E., et al, 2018a. Dioxin-like PCB 126 increases systemic inflammation and accelerates atherosclerosis in lean LDL receptor-deficient mice. Toxicol. Sci. 162, 548–558. https://doi.org/10.1093/toxsci/kfx275.

Petriello, M.C., Hoffman, J.B., Vsevolozhskaya, O., Morris, A.J., Hennig, B., 2018b. Dioxin-like PCB 126 increases intestinal inflammation and disrupts gut microbiota and metabolic homeostasis. Environ. Pollut. 242, 1022–1032. https://doi.org/10.1016/j.envpol.2018.07.039.

Plíšková, M., Vondráček, J., Canton, R.F., Nera, J., Kočan, A., Petrík, J., Trnovec, T., Sanderson, T., van den Berg, M., Machala, M., 2005. Impact of polychlorinated biphenyls contamination on estrogenic activity in human male serum. Environ. Health Perspect. 113, 1277–1284. https://doi.org/10.1289/ehp.7745.

Radomski, S.B., 2014. Update on medical therapy for male LUTS. Can. Urol. Assoc. J. 8, S148–150. https://doi.org/10.5489/cuaj.2310.

Radziszewski, P., Crayton, R., Zaborski, J., Członkowska, A., Borkowski, A., Bossowska, A., Majewski, M., 2009. Multiple sclerosis produces significant changes in urinary bladder innervation which are partially reflected in the lower urinary tract functional status-sensory nerve fibers role in detrusor overactivity. Mult. Scler. 15, 860–868. https://doi.org/10.1177/1352458509106210.

Ratliff, T.L., Klutke, C.G., Hofmeister, M., He, F., Russell, J.H., Becich, M.J., 1995. Role of the immune response in interstitial cystitis. Clin. Immunol. Immunopathol. 74, 209–216. https://doi.org/10.1006/clin.1995.1031.

Ricke, W.A., Lee, C.W., Clapper, T.R., Schneider, A.J., Moore, R.W., Keil, K.P., Abler, L. L., Wynder, J.L., López Alvarado, A., Beaubrun, I., et al, 2016. In utero and lactational TCDD exposure increases susceptibility to lower urinary tract dysfunction in adulthood. Toxicol. Sci. 150, 429–440. https://doi.org/10.1093/toxsci/kfw009.

Romero, A.N., Herlin, M., Finnila, M., Korkalainen, M., Hakansson, H., Viluksela, M., Sholts, S.B., 2017. Skeletal and dental effects on rats following in utero/lactational exposure to the non-dioxin-like polychlorinated biphenyl PCB 180. PloS One 12,. https://doi.org/10.1371/journal.pone.0185241 e0185241.

Rubin, E.B., Buehler, A.E., Halpern, S.D., 2016. States worse than death among hospitalized patients with serious illnesses. JAMA Intern. Med. 176, 1557. https://doi.org/10.1001/jamainternmed.2016.4362.

Rude, K.M., Keogh, C.E., Gareau, M.G., 2019. The role of the gut microbiome in mediating neurotoxic outcomes to PCB exposure. NeuroToxicology 75, 30–40. https://doi.org/10.1016/j.neuro.2019.08.010.

Saban, M.R., Davis, C.A., Avelino, A., Cruz, F., Maier, J., Bjorling, D.E., Sferra, T.J., Hurst, R.E., Saban, R., 2011. VEGF signaling mediates bladder neuroplasticity and inflammation in response to BCG. BMC Physiol. 11, 16. https://doi.org/10.1186/1472-6793-11-16.

Sakakibara, R., Uchiyama, T., Yamanishi, T., Shirai, K., Hattori, T., 2008. Bladder and bowel dysfunction in Parkinson's disease. J. Neural Transm. (Vienna) 115, 443–460. https://doi.org/10.1007/s00702-007-0855-9.

Sanchez-Alonso, J.A., Lopez-Aparicio, P., Recio, M.N., Perez-Albarsanz, M.A., 2003. Apoptosis-mediated neurotoxic potential of a planar (PCB 77) and a nonplanar (PCB 153) polychlorinated biphenyl congeners in neuronal cell cultures. Toxicol. Lett. 144, 337–349. https://doi.org/10.1016/s0378-4274(03)00238-8.

Sant, G.R., Kempuraj, D., Marchand, J.E., Theoharides, T.C., 2007. The mast cell in interstitial cystitis: role in pathophysiology and pathogenesis. Urology 69, S34–S40. https://doi.org/10.1016/j.urology.2006.08.1109.

Santos, J.D., Lopes, R.I., Koyle, M.A., 2017. Bladder and bowel dysfunction in children: An update on the diagnosis and treatment of a common, but underdiagnosed pediatric problem. Can. Urol. Assoc. J. 11, S64–S72. https://doi.org/10.5489/cuaj.4411.

Schantz, S.L., Widholm, J.J., Rice, D.C., 2003. Effects of PCB exposure on neuropsychological function in children. Environ. Health Perspect. 111, 357–576.

Schantz, S.L., Gardiner, J.C., Aguiar, A., Tang, X., Gasior, D.M., Sweeney, A.M., Peck, J. D., Gillard, D., Kostyniak, P.J., 2010. Contaminant profiles in Southeast Asian immigrants consuming fish from polluted waters in northeastern Wisconsin. Environ. Res. 110, 33–39. https://doi.org/10.1016/j.envres.2009.09.003.

Schnegelsberg, B., Sun, T.T., Cain, G., Bhattacharya, A., Nunn, P.A., Ford, A.P., Vizzard, M.A., Cockayne, D.A., 2010. Overexpression of NGF in mouse urothelium leads to neuronal hyperinnervation, pelvic sensitivity, and changes in urinary bladder function. Am. J. Physiol.-Regul. Integr. Comp. Physiol. 298, R534–R547. https://doi.org/10.1152/ajpregu.00367.2009.

Sethi, S., Chen, X., Kass, P.H., Puschner, B., 2017a. Polychlorinated biphenyl and polybrominated diphenyl ether profiles in serum from cattle, sheep, and goats across California. Chemosphere 181, 63–73. https://doi.org/10.1016/j.chemosphere.2017.04.059.

Sethi, S., Keil, K.P., Lein, P.J., 2017b. Species and sex differences in the morphogenic response of primary rodent neurons to 3,3'-dichlorobiphenyl (PCB 11). Toxics 6. https://doi.org/10.3390/toxics6010004.

Sethi, S., Keil, K.P., Chen, H., Hayakawa, K., Li, X., Lin, Y., Lehmler, H.J., Puschner, B., Lein, P.J., 2017c. Detection of 3,3'-dichlorobiphenyl in human maternal plasma and its effects on axonal and dendritic growth in primary rat neurons. Toxicol. Sci.. https://doi.org/10.1093/toxsci/kfx100.

Sethi, S., Morgan, R.K., Feng, W., Lin, Y., Li, X., Luna, C., Koch, M., Bansal, R., Duffel, M. W., Puschner, B., Zoeller, R.T., Lehmler, H.-J., Pessah, I.N., Lein, P.J., 2019. Comparative analyses of the 12 most abundant PCB congeners detected in human maternal serum for activity at the thyroid hormone receptor and ryanodine receptor. Environ. Sci. Technol. 53, 3948–3958. https://doi.org/10.1021/acs.est.9b00535.

Silva-Ramos, M., Silva, I., Oliveira, O., Ferreira, S., Reis, M.J., Oliveira, J.C., Correia-de-Sa, P., 2013. Urinary ATP may be a dynamic biomarker of detrusor overactivity in women with overactive bladder syndrome. PloS One 8,. https://doi.org/10.1371/journal.pone.0064696 e64696.

Singh, S., Robinson, M., Nahi, F., Coley, B., Robinson, M.L., Bates, C.M., Kornacker, K., McHugh, K.M., 2007. Identification of a unique transgenic mouse line that develops megabladder, obstructive uropathy, and renal dysfunction. J. Am. Soc. Nephrol. 18, 461–471. https://doi.org/10.1681/ASN.2006040405.

Smet, P.J., Moore, K.H., Jonavicius, J., 1997. Distribution and colocalization of calcitonin gene-related peptide, tachykinins, and vasoactive intestinal peptide in normal and idiopathic unstable human urinary bladder. Lab. Invest. 77, 37–49.

Stewart, P., Darvill, T., Lonky, E., Reihman, J., Pagano, J., Bush, B., 1999. Assessment of prenatal exposure to PCBs from maternal consumption of great lakes fish: an analysis of PCB pattern and concentration. Environ. Res. 80, S87–S96. https://doi.org/10.1006/enrs.1998.3905.

Taylor, J.A., Jones, M.B., Besch-Williford, C.L., Berendzen, A.F., Ricke, W.A., Fredrick, S. V.S., 2020. Interactive effects of perinatal BPA or DES and adult testosterone and estradiol exposure on adult urethral obstruction and bladder, kidney, and prostate pathology in male mice. Int. J. Mol. Sci. 21. https://doi.org/10.3390/ijms21113902.

Tsai, M.S., Chen, M.H., Lin, C.C., Ng, S., Hsieh, C.J., Liu, C.Y., Hsieh, W.S., Chen, P.C., 2017. Children's environmental health based on birth cohort studies of Asia. Sci. Total Environ. 609, 396–409. https://doi.org/10.1016/j.scitotenv.2017.07.081.

Turco, A.E., Cadena, M.T., Zhang, H.L., Sandhu, J.K., Oakes, S.R., Chathurvedula, T., Peterson, R.E., Keast, J.R., Vezina, C.M., 2019. A temporal and spatial map of axons in developing mouse prostate. Histochem. Cell Biol. 152, 35–45. https://doi.org/10.1007/s00418-019-01784-6.

Turco, A.E., Thomas, S., Crawford, L.K., Tang, W., Peterson, R.E., Li, L., Ricke, W.A., Vezina, C.M., 2020. In utero and lactational 2,3,7,8-tetrachlorodibenzo-p-dioxin (TCDD) exposure exacerbates urinary dysfunction in hormone-treated C57BL/6J mice through a non-malignant mechanism involving proteomic changes in the prostate that differ from those elicited by testosterone and estradiol. Am. J. Clin. Exp. Urol. 8, 59–72.

Turner, T., Chen, X., Zahner, M., Opsahl, A., DeMarco, G., Boucher, M., Goodwin, B., Perreault, M., 2018. FGF21 increases water intake, urine output and blood pressure in rats. PloS One 13,. https://doi.org/10.1371/journal.pone.0202182 e0202182.

Tykocki, N.R., Heppner, T.J., Erickson, C.S., van Batavia, J., Vizzard, M.A., Nelson, M.T., Mingin, G.C., 2018. Development of stress-induced bladder insufficiency requires functional TRPV1 channels. Am. J. Physiol. Renal Physiol. 315, F1583–F1591. https://doi.org/10.1152/ajprenal.00231.2018.

Vizzard, M.A., 2001. Alterations in neuropeptide expression in lumbosacral bladder pathways following chronic cystitis. J. Chem. Neuroanat. 21, 125–138.

von Gontard, A., Equit, M., 2015. Comorbidity of ADHD and incontinence in children. Eur. Child Adolesc. Psychiatry 24, 127–140. https://doi.org/10.1007/s00787-014-0577-0.

von Gontard, A., Baeyens, D., Van Hoecke, E., Warzak, W.J., Bachmann, C., 2011. Psychological and psychiatric issues in urinary and fecal incontinence. J. Urol. 185, 1432–1437. https://doi.org/10.1016/j.juro.2010.11.051.

von Gontard, A., Niemczyk, J., Weber, M., Equit, M., 2015a. Specific behavioral comorbidity in a large sample of children with functional incontinence: Report of 1,001 cases: Behavioral Comorbidity in Children With Functional Incontinence. Neurourol. Urodynam. 34, 763–768. https://doi.org/10.1002/nau.22651.

von Gontard, A., Pirrung, M., Niemczyk, J., Equit, M., 2015b. Incontinence in children with autism spectrum disorder. J. Pediatric Urol. 11, 261–267. https://doi.org/10.1016/j.jpurol.2015.04.015.

von Gontard, A., Niemczyk, J., Borggrefe-Moussavian, S., Wagner, C., Curfs, L., Equit, M., 2016. Incontinence in children, adolescents and adults with Williams syndrome. Neurourol. Urodynam. 35, 1000–1005. https://doi.org/10.1002/nau.22866.

Wahlang, B., Jin, J., Hardesty, J.E., Head, K.Z., Shi, H., Falkner, K.C., Prough, R.A., Klinge, C.M., Cave, M.C., 2019. Identifying sex differences arising from polychlorinated biphenyl exposures in toxicant-associated liver disease. Food Chem. Toxicol. 129, 64–76. https://doi.org/10.1016/j.fct.2019.04.007.

Wayman, G.A., Bose, D.D., Yang, D., Lesiak, A., Bruun, D., Impey, S., Ledoux, V., Pessah, I.N., Lein, P.J., 2012a. PCB-95 modulates the calcium-dependent signaling pathway responsible for activity-dependent dendritic growth. Environ. Health Perspect. 120, 1003–1009. https://doi.org/10.1289/ehp.1104833.

Wayman, G.A., Yang, D., Bose, D.D., Lesiak, A., Ledoux, V., Bruun, D., Pessah, I.N., Lein, P.J., 2012b. PCB-95 promotes dendritic growth via ryanodine receptor-dependent mechanisms. Environ. Health Perspect. 120, 997–1002. https://doi.org/10.1289/ehp.1104832.

Wu, X., Kania-Korwel, I., Chen, H., Stamou, M., Dammanahalli, K.J., Duffel, M., Lein, P. J., Lehmler, H.-J., 2013. Metabolism of 2,2′,3,3′,6,6′-hexachlorobiphenyl (PCB 136) atropisomers in tissue slices from phenobarbital or dexamethasone-induced rats is

sex-dependent. Xenobiotica 43, 933–947. https://doi.org/10.3109/00498254.2013.785626.
Yang, D., Lein, P.J., 2010. Polychlorinated biphenyls increase apoptosis in the developing rat brain. Curr. Neurobiol. 1, 70–76.
Yang, D., Kim, K.H., Phimister, A., Bachstetter, A.D., Ward, T.R., Stackman, R.W., Mervis, R.F., Wisniewski, A.B., Klein, S.L., Kodavanti, P.R.S., Anderson, K.A., Wayman, Pessah, I.N., Lein, P.J., 2009. Developmental exposure to polychlorinated biphenyls interferes with experience-dependent dendritic plasticity and ryanodine receptor expression in weanling rats. Environ. Health Perspect. 117, 426–435. https://doi.org/10.1289/ehp.11771.